Development of Novel Microfluidic Techniques for the Study of Microalgae at the Single-Cell Level

Submitted by **Sara Castillo Vila,** to the University of Exeter as a thesis for the degree of *Master of Science by Research* in Biological Sciences.

November 2021

I certify that all material in this thesis which is not my own work has been identified and that any material that has previously been submitted and approved for the award of a degree by this or any other University has been acknowledged.

Sara Castillo Vila

Abstract:

Aquatic environments make up 70% of the total Planet Earth surface and marine phytoplankton is of crucial importance in the regulation of the climate as well as a key contributor to global geochemical cycles. Although marine microorganisms have been widely studied during decades, there exists a lack of quantification methods allowing for their *in vivo* and single-cell-level investigation. The complexity of the marine environment considering currents, pycnoclines and other different physico-chemical phenomena, makes its recreation a difficult task. In order to overcome such complexities, we have studied three different microfluidic devices, here named: (i) Lagoon-like devices, (ii) Classical Mother Machine devices and (iii) Modified Mother Machine devices. Our main aim was to test the feasibility of each device in robustly growing *Ostreococcus tauri (O. tauri),* a model microalga for studies of alga-virus and alga-bacteria interactions and circadian rhythm.

We successfully followed and observed *O. tauri* development within the Modified Mother Machine microfluidic device at the single-cell level. In addition, we also investigated the different life stages of the microalgal cells with a high image resolution. We were also able to observe the proliferation of bacteria within all three devices. This fact, however, the presence of bacteria, became a problem since they inhibited the normal growth of *O. tauri* cells.

The main advantage of our system is that it allows for the long-term (up to 10 days) cultivation of single cells of the microalga under a well-controlled physical environment, as for instance: temperature, light irradiance, and medium supply.

Our system has the potential to provide a single-cell resolution to different fields within aquatic microbiology, including, cell physiology, climate change effects on individual cells and the study of microbial interactions.

TABLE OF CONTENTS

LIST OF FIGURES:

1. INTRODUCTION

1.1. Global importance of Marine Environments

Marine environments cover almost 70% of the Earth's surface and thanks to the marine currents, its waters transport heat around the globe, thus regulating climate and weather worldwide (US Department of Commerce, 2018). In 2021 the United Nations proclaimed a *Decade of Ocean Science for Sustainable Development*, a worldwide project that aims to raise awareness of the dangers that will be threating our oceans if we don't act now (The United Nations, 2021). As it is emphasised in their motto "the science we need for the ocean we want", it is essential to improve and investigate new approaches in order to conserve our oceans. There exists a reciprocal relationship between Society's health and ocean's health in which the positive or negative state of one influences the other (Nash *et al.*, 2021). In line with this, recent polls show the increasing interest of the public towards climate change and environmental sustainability (European Commission, 2021). With the pretext of such matters, Ocean Decade has been funding several programmes to value and encourage research on this topic so that the global population can benefit from our natural landscapes. It is then indisputable the predisposition and desire to investigate our largest bodies of water in the world.

Oceans are also important for life on land since they produce about 50% of the air we breathe (Simcock *et al.,* 2021). This O_2 production is due to the photosynthetic organisms that inhabit the oceans. Although historically this O_2 contribution was attributed to big plant domains (mainly macroalgae and seagrasses), it has recently been suggested that microorganisms also play a key function in O_2 production (Worden *et al.*, 2015; Venuleo, Raven and Giordano, 2017). Protistans, generally micrometric or pico-sized, are unicellular eukaryotic organisms present in considerably high concentration in the water column (Pernice *et al.*, 2014). These are varied in feeding strategies and cover a wide range of modes that includes photosynthetic, mixotrophic, parasitotics and symbiotics among others (Worden et al., 2015). The importance of such microbes along with bacteria is then broader than initially thought as they both are an important component within the network, being

part of the first links of the so-called food-web. In these regards, marine microbes were widely underappreciated and in fact, it was not until the 20th century that the concept of *Microbial Loop* was first coined by Laurence Pomeroy (Pomeroy, 1974). Briefly, the microbial loop consists of the integration and transformation of small organic and inorganic molecules into the microbial metabolism cycles so that these molecules be transformed into usable compounds to be used by other organisms placed at higher levels of the trophic web.

The microbial loop was later further explained in detail also by Pomeroy *et al.*, in 2007, who showed the existence of important relationships between different microbes and other forms of life. Life in the ocean is mainly, but not only, limited by the sunlight, nitrogen, oxygen, phosphorus, silicon and trace elements (such as vitamins) (Jeffrey S. Levinton, 1995). Sunlight is present in the so-called photic zone, which depending on the specific area and the water characteristics, can reach a depth of 200 meters (Costello and Breyer, 2017). Strict photosynthetic (photoautotrophs) organisms depend solely on this factor to grow. For instance, *Cyanobacteria*, a group previously known as blue-green algae, are a type of bacteria capable of carrying out photosynthesis as a result of the existence of different forms of chlorophylls. This group is considered an important primary producer and thus is usually placed at the base of the trophic web. Picoplanktonic species, such as *Synechococcus* and *Prochlorococcus* are dominant cyanobacteria and studies suggest that they account for more than half of the marine photosynthesis (Jeffrey S. Levinton, 1995; Garcia-Pichel *et al.*, 2009). In addition to *Cyanobacteria*, diatoms and dinoflagellates (in the *Ochrophyta* and *Miozoa* phyla respectively) are also of interest in marine primary productivity, being the most abundant groups within the phytoplanktonic group (Depauw *et al.*, 2012; Rodrigues, Patil and Anil, 2022).

However, the presence of organic and inorganic compounds is also of crucial importance. The microbial loop in fact, considers the exchange and recycling, and the processing of this organic and inorganic matter by bacteria to be further recycled by the phytoplankton and vice versa. This phenomenon, occurring within the microbial loop, is presented in **Figure 1**, adapted from Worden *et al.,* 2015.

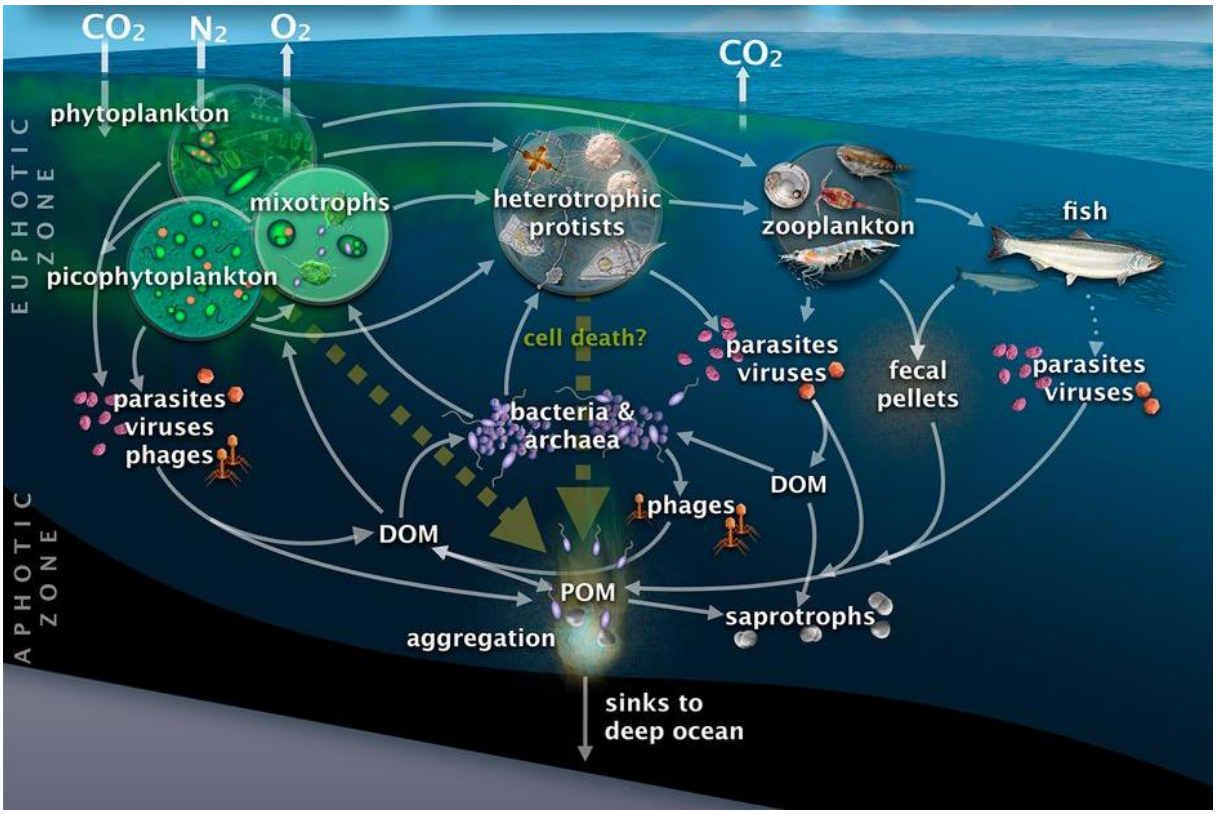

Figure 1. *Oceanic food-web structure. DOM and POM are dissolved and particulate organic matter respectively. As can be observed, eukaryotes are present throughout all the interactions, whilst prokaryotes are found just at the bottom layer. The result is, as observed, the creation of a cycle where particles flow between groups in the water column and to the sediments. Adapted from Worden et al., 2015.*

As observed, there exists a network of interactions where the organic matter produced, exudated or excreted by bacteria and archaea is then processed and converted into energy that can be later recycled by phytoplankton and heterotrophic protists. The magnitude of the microbial loop goes beyond microbes since ultimately, such matter and nutrients reach other groups of zooplankton, giving structure and stability to marine ecosystems (Azam *et al.*, 1983).

Incorporating the above-mentioned knowledge about the microbial loop, changed historic knowledge about primary productivity in the ocean and it also affected the way marine microorganisms were to be studied.

1.2. The Phycosphere and The Microbiome

Microorganisms make up approximately 70% of the total marine biomass forming the microbiome (Bar-On, Phillips and Milo, 2018). These microorganisms play an essential role in the maintenance and stability of the marine food web as well as in global nutrient cycles (Seymour *et al*., 2017). Because of their crucial role in marine PP, efforts to understand how microbial interactions may influence PP have been made, for instance bacteria directly interacting with eukaryotic algae. In this context, we should refer to the so-called phycosphere, which is defined as the region immediately surrounding individual phytoplankton cells (from Seymour *et al.*, 2017). It is believed that it is in this region where interactions between bacteria, algae and viruses take place. Such interactions can involve the exchange of different substances, however the most common is that of micronutrients such as vitamins metabolites (Cooper *et al*., 2019).
As pointed out by Variem and Kizhakkedath (2021), the most predominant component within the phycosphere are prokaryotes including bacteria. Consequently, the study of the interactions occurring within the phycosphere, have usually been complemented by the investigation of the microbiome, a field of study that has been on the rise since 2006 (Donachie *et al.*, 2021). In fact, some studies have shown that interactions taking place within the microbiome can affect the health and stability of both algal and bacterial cells, influencing ultimately, the structure of the communities involved in the interaction (Boon *et al.*, 2014; Longford *et al.*, 2019). In order to study the phycosphere and the microbiome, an organism frequently used as a model system is the green alga *Ostreococcus tauri* (*O. tauri*), the tiniest (<2µm) free-living eukaryotic cell (Chretiennot-Dinet *et al.*, 1995). *O. tauri* has been used as a model organism due to its compact genome, small size, and thus simple physiology, and due to its manageable culture conditions (Lelandais *et al.*, 2016). It was firstly discovered in the Thau lagoon (connected to the Mediterranean Sea) in 1994 and yet, its role and interactions with other microbes have not thoroughly been identified (Abby *et al*., 2014). Great efforts are being made in the field, which will allow the understanding of *O. tauri*'s role within the marine environment and its relationship with other bacterial and viral communities (Clerissi, Desdevises and Grimsley, 2012). Cooper *et al.*, in 2019 pointed out a mutualistic interaction between *O. tauri* and bacteria (*Dinoroseobacter shibae*), where both algae and bacteria benefited through a cross-

exchange of B-vitamins. Other studies have shown how in this interaction bacteria could potentially be promoting algal growth, as already assessed for terrestrial plants (Ramanan *et al.*, 2016; Hakim *et al.*, 2021). Abby *et al*. (2014) analysed the gene content of the microbial community associated with *O. tauri,* showing the presence of reference genes which play a major role in symbiotic associations. Once more, similarities with terrestrial systems' rhizospheres were found, suggesting that there could be specific secretion systems in the microbiomes involved in cell-cell interactions with *O. tauri* (Abby *et al.*, 2014). How specific these interactions are is still a matter of debate; it has been demonstrated for some species of green algae that interactions are indeed species dependent (Kim *et al.*, 2014; Ramanan *et al.*, 2015). Another study made use of metagenomic and RNA-Seq data to discover that certain strains of the *Chlorella*, *Scenedesmus* and *Micrasterias* genera had unique phycospheres composed of specific microbial communities (Krohn-Molt *et al.*, 2017). In these terms, metagenomics consists in the study of the total genetic material within a mixed community (Gilroy *et al.*, 2021) and RNA-Seq uses high throughput sequencing methods to analyse the transcriptome of a given cell (Kukurba and Montgomery, 2015). Yet, due to the small size of the organisms within the microbiome, one of the main problems when working with it is that it is not easy to address with the current technical methodologies. Therefore, the nature of such relationships cannot still be fully understood.

1.3. Traditional and Current Methodologies to Study the Phycosphere

Due to the extreme physical conditions (e.g., pressure, salinity, and temperature), characteristic of the aquatic environment, the study of microorganisms is highly dependent on the advances in technology. Traditionally, techniques to study microbes and their relationships with other organisms mainly involved simple methods such as culture and subsequent total growth count in Petri dishes or direct visualization under a microscope (Lasken and McLean, 2014). Along with these techniques, the invention of the spectrophotometer in 1939 whose technical principle was based on the interaction of the radiation with atoms, ions, and molecules (Frenzel and McKelvie, 2008), was a milestone in the investigation of samples from aquatic environments. At the present time,

the study of marine microorganisms entails a problem since most of them are unculturable. One of the direct consequences of this fact is that techniques commonly used to study them are molecular-biology based such as sequencing and culture-independent based techniques (Farinas *et al.*, 2006; Depauw *et al.*, 2012). Such techniques are the most reliable ones if phylogenetic or transcriptomic analyses, amongst others, are the aim. Yet, they are often time consuming and generally require the use of expensive and harmful reagents and machinery. Moreover, the need of qualified personnel not only to execute them but also to analyse the results is frequently an impediment (Son, Brumley and Stocker, 2015). Another handicap found in sequencing approaches is that they rely on reference genes, which for most marine microorganisms have not been determined yet (Monier, Worden and Richards, 2016; Pachiadaki *et al.*, 2019). In addition, the beforementioned techniques rely on ensemble measurements and therefore do not allow for the study of the behavioural traits of the individual cells. Especially relevant are the approaches that have been used to study the microphytoplankton and bacterioplankton as they are our case of study. For example, Sebastián and Gasol in 2019, wrote a review where they highlighted how decisive it is to complement “omics” techniques with observational approaches on microbial ecology. They show examples where greatly entrenched hypothesis were modified thanks to the combined use of Bio-Orthogonal Non-canonical Amino acid Tagging (BONCAT) along with Raman spectroscopy among others. Another recent paper did a review on the technologies currently available to study particles of varied sizes, from microns to centimetres in the aquatic environment (Lombard *et al.*, 2019). As they remarked, the importance of visualizing these particles is vital to better understand some of the most important processes: biogeochemical cycles and sediments’ decantation, for example. Moreover, they concluded that the study of such particles, ranging from <2 um (picoplankton) to 2000 um (macroplankton) (Finkel *et al.*, 2010), is still a challenge and innovative technologies are needed to advance our knowledge of marine biology. Since 80-90% of the phytoplankton is between the size of 0.2 um and 3 um (Massana, 2011), it is coherent to treat these organisms as particles and to actively develop new tools to study them. Within this framework, single-cell level investigations face a huge challenge in the marine biology and ecology field.

Current approaches for single-cell studies are, once more, molecular biology based which is not a disputed point, but they often provide a limited output, as for example, incomplete transcriptome or bias to nucleic acid amplification. Thus, areas such as physiology, cell morphology and ecology are left uncovered with the techniques currently available. Hence the need to apply new procedures and state-of-the-art technologies at the single-cell level to allow real-time and *in vivo* observations. However, it is worth mentioning that the complementary use of molecular tools with direct observation techniques is and will be a breakthrough for diverse areas within the scientific community. Within the techniques historically and still currently employed are those based on the physical and chemical characteristics of the particles themselves and not in the physiological or structural characteristics of the cells. The dominant approach in this field is flow cytometry: when a particle moving in a liquid stream is exposed to a laser beam, the light is then scattered in different angles, giving information about the cell diameter, surface roughness and fluorescence (Mandy, Bergeron and Minkus, 1995). Flow cytometry is often used in single-cell analyses for cell counting, cell sorting, cell viability, cell pigments and cell adherence among other parameters (Anderson, 2005). Due to the nature of flow cytometry, highly dependent on the physicochemical characteristics of the sample, its application to investigate further marine microorganisms carry some disadvantages: first, the form in which light is scattered to determine the sample does not apply uniformly to all cell shapes. In addition, cells without pigments need to be stained, otherwise they are not detectable by the lasers incorporated in the flow cytometer, and thus cannot be processed *in vivo*. Second, it uses single particles and if they are very small (e.g., < 2 um), the cytometer is unable to distinguish between them creating a bias in the results (Hildebrand *et al.*, 2016); third, samples are, in some cases, lost after analysis due to the pre-treatment needed to fix the samples (destructive technique); and last, it does not give a detailed information about the physiology or cell morphology of the organisms (Spencer and Morgan, 2011; Vembadi, Menachery and Qasaimeh, 2019).

Technological advances and improvement of sample preparation have allowed the emergence of new techniques to study at the single-cell level, for instance bioimaging and microscopy. These have shown the potential to shed light into the physiological and phenotypical traits of microorganisms. Single-cell imaging has widely been used to

determine cellular parameters such as cell organization, cell division and host-pathogen interactions during infections (*Single-cell microbiology*, 2016) and it is often aided by genetically modifying the microbe under investigation to constitutively express fluorescent proteins. Furthermore, live-cell imaging can be further aided by the use of microfluidics that facilitate single-cell tracking over an extended period of time (Bamford *et al.,* 2017) (please see next section). Alternatively, in electronic microscopy (both, Transmission and Scanning), sample processing is arduous and requires pernicious and expensive chemical compounds. Besides, if the sample has initially been kept in liquid, the resolution of the images acquired is poor, since TEM and SEM work under a high vacuum atmosphere during operation, which can potentially suck the aqueous part of the cells themselves, destroying them (Mielańczyk, Matysiak and Wojnicz, 2015). Despite these drawbacks, the ultrastructure of *O. tauri* was determined using these microscopes. It was achieved by Henderson, Gan and Jensen in 2007 using electron cryotomography. As a result of using this technique, they effectively imaged *O. tauri* throughout every stage of its life cycle for the first time. Cryotomography needs the sample to be frozen initially and thus they imaged and composed the final images where the specific structures of the cells can be observed in detail. This study shed light on the way *O. tauri* divides as they were able to observe the cells in distinct phases and they even captured the organelles in the middle of division.

1.4. Microfluidics

Microfluidics is an emerging technology that involves the study of physical and biological processes at the microscale. A typical microfluidic system takes into consideration the physicochemical characteristics of a fluid which is subjected to high pressures, usually generated by the micro-scalation process. As a part of the micro-scalation process, specific devices are designed to have a width and height between 100 nm and 100 um (Convery and Gadegaard, 2019). It originally started with the development of microelectronics when photolithography was developed for the first time. Parallel to this invention, the inkjet printing was created and soon it became a revolution as materials more affordable such as silicon became popular. This marked the beginning

of microfluidics as we know it today. The combination of photolithography and etching techniques, that used new materials, were investigated and the application to these new materials to fluids opened a new path within science. Soon, the small size of the microchips, still made of silicon, was undoubtedly decreasing the volume of reagents used for investigation which was seen as an advantage in several areas of the applied sciences.

One of the first fluids that were used to test the microchips was a gas and was applied to gas chromatography (Terry, Herman and Angell, 1979). They used a chip fabricated in silicon using photolithography and chemical etching and it initiated what today is recognized as “Lab on a Chip”. Ten years after this technique came to the fore, and through a process of technological advances, the μ-TAS (miniaturised Total Analysis Systems) concept appeared. The name came from the idea that multiple variables were able to be analysed using one single device. One of the main characteristics of the μ-TAS is that the devices included different detectors and analysers functioning at the same time and in a same sample, which allowed the processes to be automatized, hence becoming more efficient and accurate (Convery and Gadegaard, 2019). Moving forward in time (**Fig. 2**), microfluidics systems became popular in different knowledge areas which, along with several technological advances, culminated with the creation of a consolidated new science as we understand it today. After the 2000´s, the application of microfluidic systems to cell culturing became a standard practice. One of the compounds that revolutionized the field was PDMS (Polydimethylsiloxane), introduced by Whitesides in 1998 (Duffy *et al.*, 1998). It resulted in a huge step forward because of its physicochemical properties as a polymer, for example: interfacial free energy, gas permeability, thermal stability, and transparency, which facilitated the handling of microfluidic systems to a substantial extent (Gale *et al.*, 2008). For this reason, the use of PDMS became the standard and almost all areas within biological sciences that made use of microfluidics, operated with such a compound (Massalha *et al.*, 2017; D. Yang *et al.*, 2018). The manufacturing and operating process of microchips has been widely referenced (Fredrickson and Fan, 2004; Dervisevic *et al.*, 2019; Nguyen *et al.*, 2019). Briefly, to obtain a microfluidic system, first a mould is needed, generally made of silica, this is the negative of the device of interest. In order to obtain the functional device, the silica mould is filled

with liquid PDMS and needs to be cured in the oven. Later it is separated from the mould and separated into individual units, thus obtaining our device.

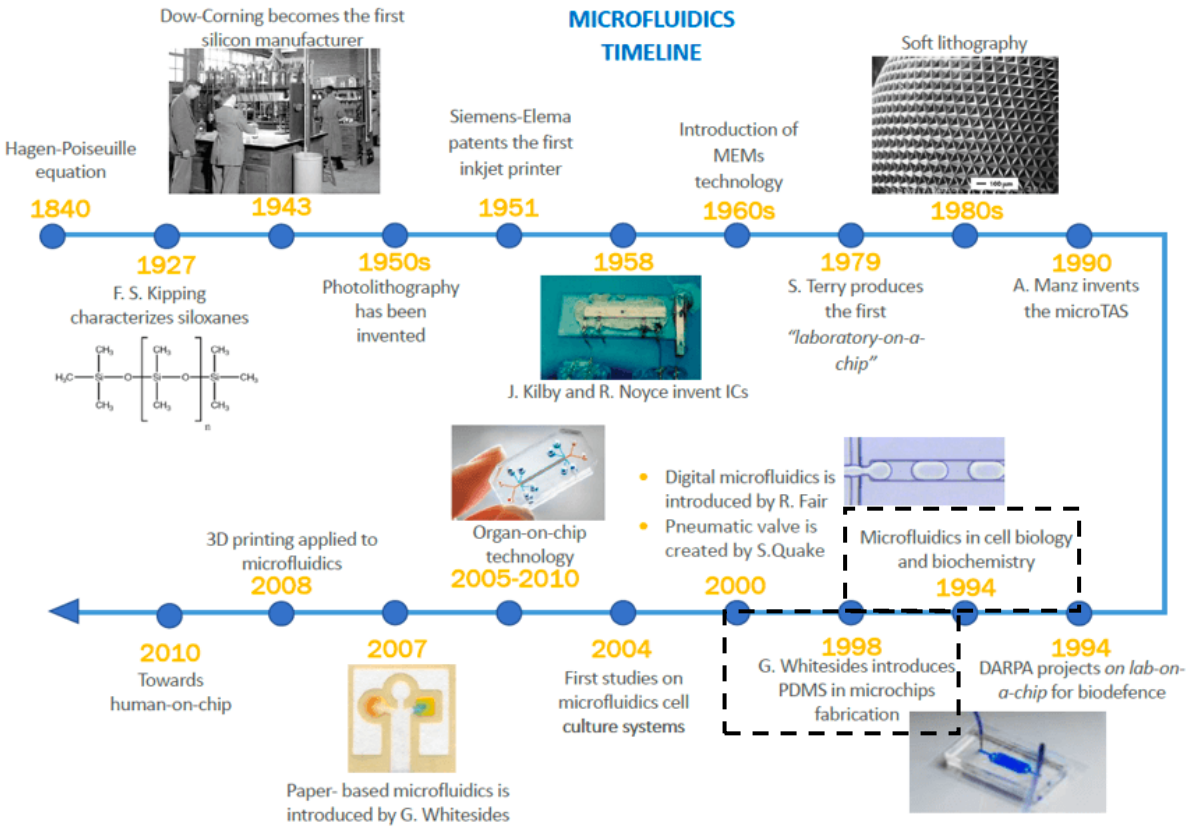

Figure 2. *Main advances during the development of Microfluidic Technologies. Particular attention is to be paid in the application of microfluidics to Biological Sciences in 1994 and the discovery of PDMS applied to microfluidics in 1998 (black dashed rectangles respectively). Picture retrieved from: https://www.elveflow.com/microfluidic-reviews/general-microfluidics/history-of-microfluidics/ (Accessed on the 21st August 2021).*

To obtain maximum performance out of microfluidics, devices are complimented through the connection of external adds-on such as portable syringe pumps, microscopes, and thermal chambers, among others. The sum of all these small advances led to the current panorama: modern microfluidics. As well discussed above, the medical research field soon made use of this novel technique, and even at this moment, microfluidic applications include different areas within the biophysical field, including the fight against antimicrobial resistance (AMR) (Baltekin *et al.*, 2017; Bamford *et al.*, 2017; Birkhofer *et al.*, 2018; Burmeister and Grünberger, 2020; Cama *et al.*, 2020; Goode *et al.*, 2021; Hammond *et al.*, 2021; Łapińska *et al.*, 2021; Dimitriu *et al.*, 2022; Glover *et al.*, 2022). A good example of this that changed the way AMR was studied was the creation of what is known as the *Mother Machine* device in 2010 by Wang *et al*. They presented an innovative microfluidic device which allowed the study of the growth and division patterns of *Escherichia coli* by observing the mother cells *in vivo* under a fluorescence microscope (**Fig. 3**). The mechanism within the device, as observed in figure 3, consisted

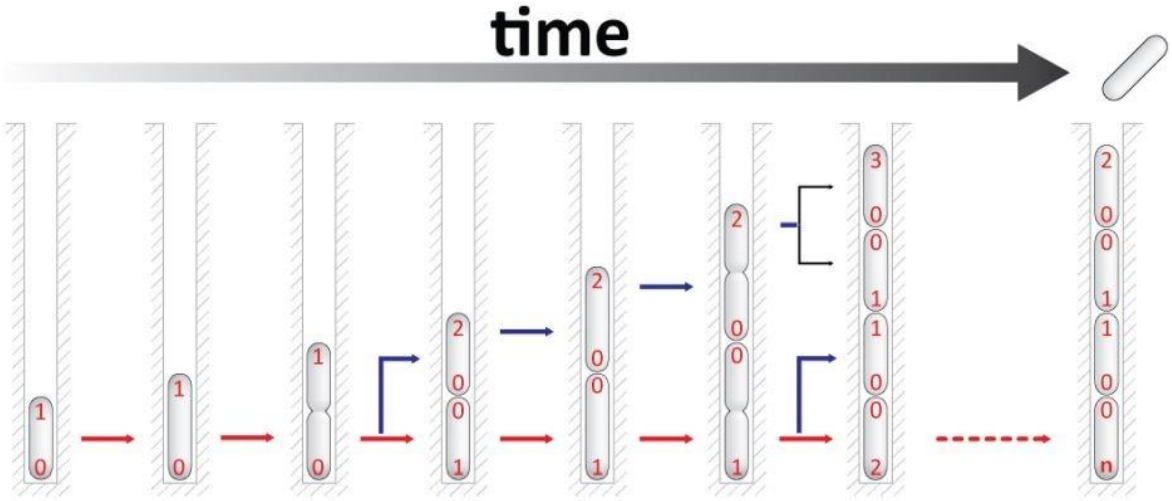

Figure 3. *Growth channels (or arms) within the Mother Machine device. As observed, an initial Mother Cell is loaded into the arms and its division pattern can be followed through time. Model given for* E. coli*. The upper part of the device, where the time arrow is, is where the main channel would be placed, and it is in such a channel that the medium reaches each of the arms by diffusion. Such diffusion allows for the renewal of the medium at all times. Retrieved from Wang* et al.*, 2010.*

of several confinement spaces (arms), where individual cells were trapped by diffusion. This system was also supported by an additional syringe pump which provided fresh media to the device and an incubation chamber to maintain the temperature steady for the duration of the experiment (Wang *et al.*, 2010).

As a result of the creation of the *Mother Machine* device, the study of *E. coli* and other microorganisms, such as yeast cells, at a single-cell level became a reality (Jo and Qin, 2016; Łapińska *et al.*, 2019; Reinmets *et al.*, 2019; Hammond *et al.*, 2021; Glover *et al.*, 2022). Understanding how a single cell behaves has deep implications in ecology since the vast majority of the microbial communities are heterogeneous (Hodzic, 2016).This means that despite what can be understood as a collective reaction, in reality there is found a hidden individual mechanism that varies with the specific genotype and phenotype of each cell involved in the overall response (Kaiser *et al.*, 2018). However, despite microfluidics' emergence at the end of the last century, it was not until recent years that the microfluidic techniques began to be used in other areas such as marine biology. Due precisely to this late application within this area, the challenges we face today are still considerable and require new protocols and techniques. Hitherto, marine organisms used in this field have, once more, been applied in the medical research to answer questions rather related to human's diseases more than to study their own ecology. However, the application of microfluidics to investigate and to better understand marine ecology or more specific areas within the aquatic environment have not yet been exploited. Notwithstanding, the examples we currently have are a satisfactory proof of concept that have paved the way for a more extensive use of microfluidics broader than bacteria. These systems started with model organisms such as Zebrafish (*Danio rerio*) to study embryonic development and toxicology (Funfak *et al.*, 2007; Zhu *et al.*, 2015; Khalili and Rezai, 2019a). Such toxicological studies with zebrafish showed immense potential to study other ecological parameters and thus the use of marine microorganisms began to become popular.

1.5. Microfluidics Used in Marine Biology: Actual Status.

Ramanathan *et al*. (2013) presented for the first time a microfluidic-based tracking system to study plankton and its response to environmental changes, and this was achievable due to the investigations executed years before where the first marine organisms were used, still for biomedical discoveries (*See Section 1.4*). However, the latter study laid the foundations in terms of designs, flow-through systems, and image analyses to analyse different environmental variables that quickly were appropriated and applied in drug discovery. This study (Ramanathan *et al.*, 2013) made use of *Platynereis dumerilii*, a species of annelid polychaete (part of the zooplankton), that has widely been studied and is currently a settled model organism. It is a ubiquitous species and as such it is found in every marine environment around the world. Its ease for cultivation is well known and due to this fact, studies with microfluidics have often involved the analysis of the effects to environmental changes on them. Along with these studies, behavioural investigations on *P. dumerilii* have often been carried out using microfluidics by physical confinement within the microchips(Ramanathan *et al.*, 2015; Chartier *et al.*, 2018). Yet, such confinement was created so that the annelid had enough space to freely move inside the allocated space.

Surprisingly, only the three aforementioned papers used microfluidics to observe *in vivo* the behaviour of *Platynereis* sp. when exposed to a changeable medium. They tested different pH conditions and studied the behavioural changes at a single-cell level. They designed two different microfluidic devices, one of which enabled the creation of pH gradients along the chip; the second was created to observe the movement through different streams, aiming to mimic the natural habitat of *P. dumerilii*, the intertidal sediments (Ramanathan *et al*., 2013). Using a camera to track *P. dumerilii*, they were able to analyse parameters such as overall speed, time of movement and time of adaptation to such changes and, the specific movements along the streams (Ramanathan *et al.*, 2013). This same group analysed, a few years later, with the same device, the responses to pH changes in order to determine the ecological *preferendum*, obtaining as a result a quantified pH concentration for the individuals to elicit a response. Thanks to this investigation, chemosensing-triggered behaviours within this planktonic group were

elucidated and microfluidics re-established itself within the biological field. Another recent paper on *P. dumerilii* using microfluidics (Chartier *et al.*, 2018) used a slightly different approach, as in this case, the juvenile polychaete was immobilised with no free-swimming movement in the microchip. Chartier *et al.*, in 2018 successfully combined the microfluidic system with calcium imaging in order to determine the chemosensory activity of the neurons.

Another well studied model organism from the planktonic group is the larvae and embyros of *Danio rerio* (commonly known as zebrafish), a fish from the *Cyprinidae* Family, whose importance goes beyond marine ecology (Tang *et al.*, 2015; Choi *et al.*, 2021; Sullivan *et al.*, 2021). For investigations making use of microfluidics, this fish is used in its embryonic and/or larval stages, and the parameters investigated the most are hereditarian, and the neurological and behavioural bases of diseases as well as toxicological and drug screening assessments (Zhu *et al.*, 2014). Predictably, depending on the variable of interest, the design of the microfluidic device varies. At the beginning, the approach used was what is known as microfluidic segment techniques (Huebner *et al.*, 2007), this employed Teflon®, a transparent and chemically inert and non-toxic material, tubing coil that was supplied with a fluid with a high density mimicking the blood, the embryos were then loaded and imaged in each of the segments that were created by the creation of air bubbles within the tube (Funfak *et al.*, 2007). Unlike the devices presented to study *Platynereis*, most of the analyses on zebrafish allowed for the free movement of the specimen during the experiments. However, it is worth mentioning that the immobilisation of zebrafish is also a prevalent goal since physiological characteristics are better observed when the fish, already in its juvenile stage, is motionless. This aim has influenced the way devices are designed, usually creating two differentiated spaces within the chips, one for the larval stage and another one for the juvenile stage, both connected through channels (Khalili and Rezai, 2019b). Hereupon, the microfluidic devices presented for the study of zebrafish are more versatile and varied, for instance, the incorporation of 3D printed devices is also a reality (Zhu *et al.*, 2015) **(Fig. 4).**

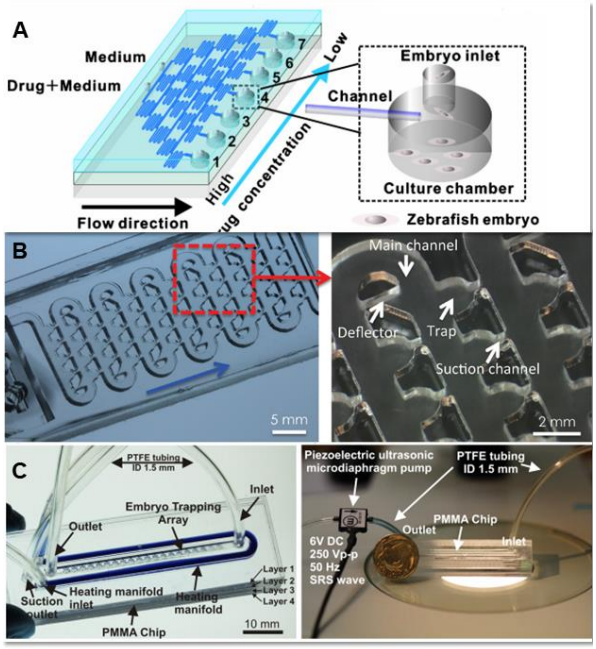

Figure 4. *Most relevant devices to study* Danio rerio.

A: Integrated array microfluidic device to analyse zebrafish embryos made of glass. As observed in the image, they integrated 3 different layers (three of them glass) in order to create a drug concentration gradient. They evaluated the developmental toxicity and teratogenicity effects of drugs on zebrafish embryos. (Retrieved from Yang *et al*., 2011)

B: Microfluidic device for embryo trapping and immobilisation. Master mould was made of PMMA (poly-methyl methacrylate) and replica moulding was carried using PDMS. Such PDMS replicas was then bond to glass slides for observation under the microscope. They developed an automated system to manipulate and to analyse zebrafish for drug discovery. (Retrieved from Akagi *et al*, 2012).

C: Integrated 3D microfluidic devices made of PMMA. Multiplatform device consisting in 4 different modules, including embryo loading channel, mechanical trapping zones, suction manifolds and heating manifolds to warm the surrounding water. They created an automated system to trap single embyros for the investigation of pharmacological agents. (Retrieved from Akagi *et al*., 2013)

All three devices presented in **Fig. 4** were originally designed to study pharmacology, drug discovery and molecular medicine, thus they aimed to cover variables related to embryo development in different arrays. Therefore, all three were built using transparent materials and drug supply was assured by the implementation of inlets and outlets where tubing was connecting the chips to the syringe pumps or other software-controlled devices that allowed the continuous flow of media.

Draw from the premise that the marine environment is fluid, it was only a matter of time until microfluidic approaches started to be applied in marine ecology. When considering marine microorganisms for use in microfluidics, it is relevant to distinguish between active swimmers and non-active simmers. Both are present in the water column, and they belong to both zooplankton and phytoplankton components (Michalec *et al.*, 2017; Wirtz and Smith, 2020). The significance of distinguishing between the two groups is due to the fact that depending on which group they belong to, the design of the chips will be adapted to one or another way of living, as already observed for *D. rerio*. In

addition, microfluidics implies a substantive change in marine microbiology in comparison with traditional techniques, since culturing techniques do not allow the growth of all bacteria present in a sample. Bacteria viable but not cultivable is a well-studied phenomenon (Bamford *et al.*, 2017) characterized by the lack of growth of bacteria using conventional methods. This is the case also for marine bacteria, and for all the marine microorganisms in general, since the recreation of the marine environment is not always achievable (Zhang *et al.*, 2021).To overcome this limitation, microfluidics offers a useful approximation to the aquatic environment by the creation of different fluid regimes present in the natural habitat (White, Jalali and Sheng, 2019). In this line, Son, Brumley and Stocker in 2015, studied the motility of different marine bacteria using imaging-microfluidics systems, they investigated diverse strategies bacteria may acquire depending on their physiological structure. For instance, they studied the mechanical function of the flagella of marine microbes under chemotaxis, when in a changeable fluid environment. Other studies from this group have also focused on bacterial resistance to antibiotics, nonetheless, they were pioneers also in marine microbial ecology studies using microfluidics (Seymour *et al.*, 2010, 2017; Rusconi, Garren and Stocker, 2014).

Another advantage proposed by microfluidics in this discipline is the observation and investigation of cell-to-cell interactions. This combination of single-cell level studies and microfluidics was the stimulus for conducting this project. Bibliographic reviews showed that there was a considerable potential to apply all the above-mentioned techniques to marine microphytoplankton and there existed a clear lack of investigations in this direction. What is more, the studies found revolved around biotechnology with a clear goal: to mass produce certain microalgae species that had already been successfully grown for their commercialization, thus not studying at the single-cell level (Ramanan *et al.*, 2016; Kim, Devarenne and Han, 2018; Bodénès *et al.*, 2019). **Fig. 5** shows different microfluidic devices that have been used for the growth of microalgae. As observed in figure 5, the most important aspects considered for the creation of the devices are not those of design anymore, but instead they focus more on the appliances that can be added to the microfluidic chips. In this sense, different sets of laser beams, filter and lights are used in order to maximize the algal growth depending on the aim. Hashemi *et al.*, in 2011 (**Fig. 5**, **A**) created a “micro-flow cytometer” to test the variability in fluorescence

within the same algal community, whose results were used afterwards to characterize down to specific algal strain. They aimed to create a device that could accurately be used for in-field research. As discussed in their work, most of microfluidic devices currently available are composed of several parts which implies the devices can only be used in a specific facility and their creation often requires arduous lab protocols and skilled personnel (see, for example: (Sato *et al.*, 2007; Golden *et al.*, 2009; Rosenauer *et al.*, 2010). Similarly, Schaap, Rohrlack and Bellouard, in 2012 (**Fig. 5**, **B**), based on the same principles as in Hashemi *et al.*, (2011), they presented an optofluidic device for identifying algal species. In this study, their device not only allowed for the identification of algae, but it also could distinguish between particle sizes within a mixture which allowed for the identification of individual strains. The main difference between both systems (**Fig. 5 A** and **B**) is that the latter would need to adapt several changes in order to be functional in an outdoor environment. The device in **Fig. 5 C** instead was developed to investigate the phototactic response of the algae. The design of the chip is slightly different to those in **A** and **B**, as it consists of two reservoirs, one for loading the sample and one for the algae to move as a result of a response to the light they are exposed to in the first chamber. Their specific aim was to measure the speed of such movement in terms of photosynthetic efficiency. They used the green alga *Chlamydomonas reinhardtii*, used mainly as a model system to investigate biotechnological applications of algae for biofuel and bio-products within industry (Scranton *et al.*, 2015; L. Yang *et al.*, 2018; Banerjee, Ray and Das, 2021). Hence the importance of discovering ways to enhance its production by determining its maximum photosynthetic efficiency. In contrast to the other two studies, apart from testing their hypothesis, they also carried out genetic analyses of the isolated strains in the interest of obtaining a better knowledge on the specific traits that influence the greater growth of the algae, thus allowing for further genetic engineering and commercialisation.

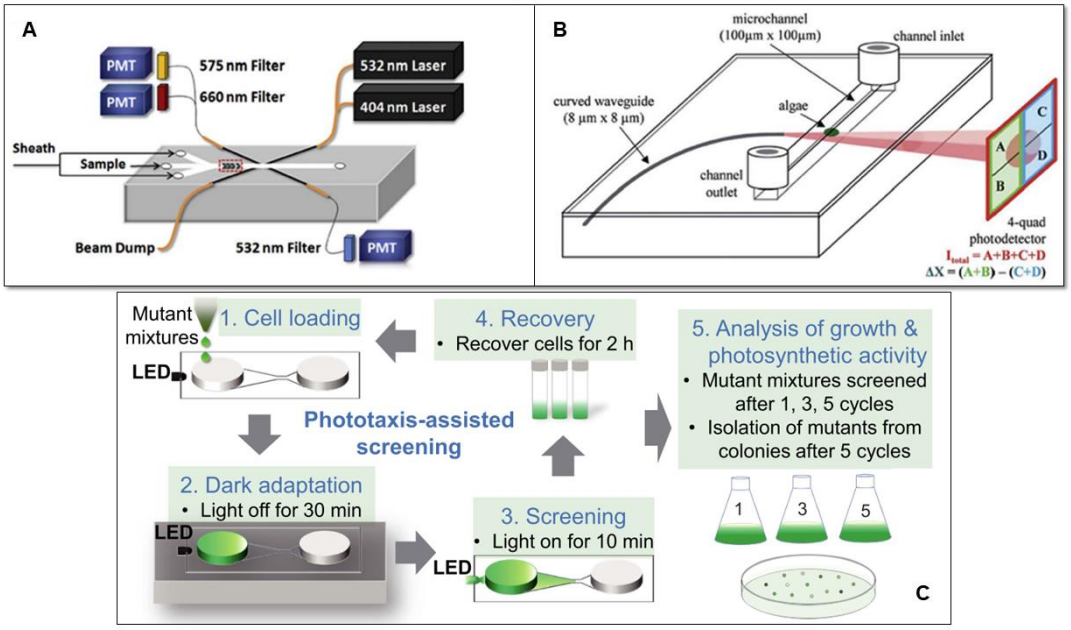

Figure 5*. Integrated microfluidic platforms and devices that have been used to study different strains of microalgae.*

A: PDMS chip for characterization of marine microalgae using optical physics. Specimens analysed: Karenia b., Synechococcus sp., Pseudo-Nitzchia, and Alexandrium. Retrieved from Hashemi et al., 2011.

B: Glass chip for optical classification of microalgae species. Specimens used: Cyanothece aeruginosa, Scenedesmus acuminatus, Chlorella vulgaris, Microcystis viridis, Anabaenopsis sp., Navicula pelliculosa, Pseudokirchneriella subcapitata, Pseudanabaena sp., Monoraphidium griffithii. Retrieved from Schaap et al., 2012.

C: PDMS-based chip to analyze single-cell phototactic responses in Chlamydomonas reinhardtii for further isolation. Retrieved from Kim et al., 2016.

1.6. Single-Cell Microfluidics Research Applied to Microalgae.

Thus far, different microfluidic approaches for marine organisms' cultivation have been introduced. Yet, examples making use of microalgae did not work at the single-cell level, nor were focused in answering ecological questions (Scranton *et al.*, 2015; Bodénès *et al.*, 2019).Since that is precisely the perspective we wanted to study, we reviewed the available methodologies in this subject, and, surprisingly, there were only a few published works focussing on single-cell growth of microalgae within marine ecology. In 2016 Luke *et al.*, developed a platform that allowed the visualization of different algal strains at a single-cell level. The microfluidic system was integrated into an inverted fluorescent microscope, where images were taken every 5 min, creating time lapses that were further analysed using a cell tracking algorithm (**Fig. 6**).

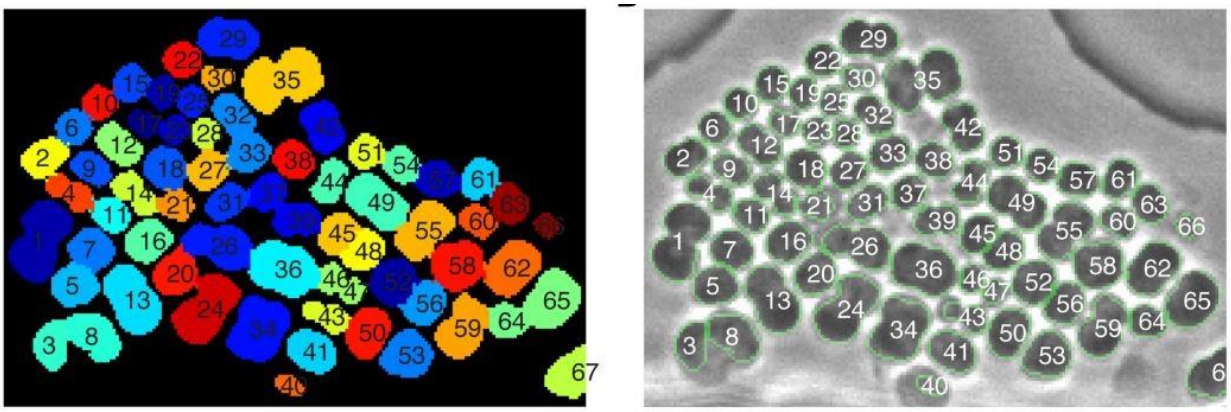

Figure 6. *Image analysis prepared using a tracking algorithm developed by Luke et al,. 2016 to be implemented in the software ImageJ. In this figure, the growth of the cyanobacteria* Synechocystis *is shown. Numbers refer to the progression of growth from a first cell. The algorithm also allowed for the measurement of the area of each of the cells imaged. Retrieved from Luke et al., 2016.*

Thanks to this tracking system, and the continuous supply of fresh medium, they determined and followed the growth rates and division patterns for up to 68h of a group of algal cells. In addition, this system allowed for changes in the medium supplied and thus they were able to observe the natural responses of the individual cells when creating an environment with fluctuations in, for example, changes in nitrogen supply. Their

microfluidic devices were made of PDMS and bonded to glass coverslips. The devices consisted of several circular cell chambers (**Fig. 7**, **A** and **B**) where the cells were trapped using a syringe pump.

Since the marine environment is highly changeable, when designing an experiment, it is important to consider long cultivation time periods in order to capture different phenotypic changes that could happen in the natural habitat. The study from Luke *et al.*, in 2016 is a clear example of how microfluidics can be applied to aquatic microbial ecology to track algae at the single-cell level. Investigations studying ecological issues are mainly focused on light absorbance and thus photosynthetic efficiency of algae. For this reason, a great emphasis is put on illumination methods, which inherently also involves the nature of the materials for the fabrication of the microfluidic devices (Kim, Devarenne and Han, 2018). Throughout the first sections, the compounds used to fabricate the devices varied to a large extent, both in design and manufacturing, whilst in this specific area, microfluidics applied to microalgae, the most successful material has so far been PDMS, precisely because of its characteristic transparency. To conclude with the most recent techniques, the following figure **(Fig. 7**) shows devices that have successfully been used to analyse microalgal growth at the single-cell level and applied to ecological concerns. However, none of them made use of *O. tauri*.

Wang *et al.*, (2016) created the device illustrated in **Fig. 7**, **C**. The device was made of PDMS and bonded to a glass-slide. However, the trapping technique in their device varied from that found in most microfluidic devices. They induced the creation of an air bubble where the cells were captured on the surface of the bubble. The air bubble originated from the formation of a gas-liquid interface within a liquid environment. In order to improve and to produce a reliable method, they evaluated the cells capturing efficiency of their microfluidic device. To this end, they analysed the different pH ranges in which algal cells do not change their surface chemical charge, because such change could influence the electrostatic repulsion forces, hence affecting the attachment of the cell to the air bubble within the system. The optimum pH was determined based on the photosynthetic activity measured by autofluorescence intensity of the microalgae. Finally, they developed a method to track and to study microalgal cells at a single cell level and with the possibility to expose the cells to different environmental conditions.

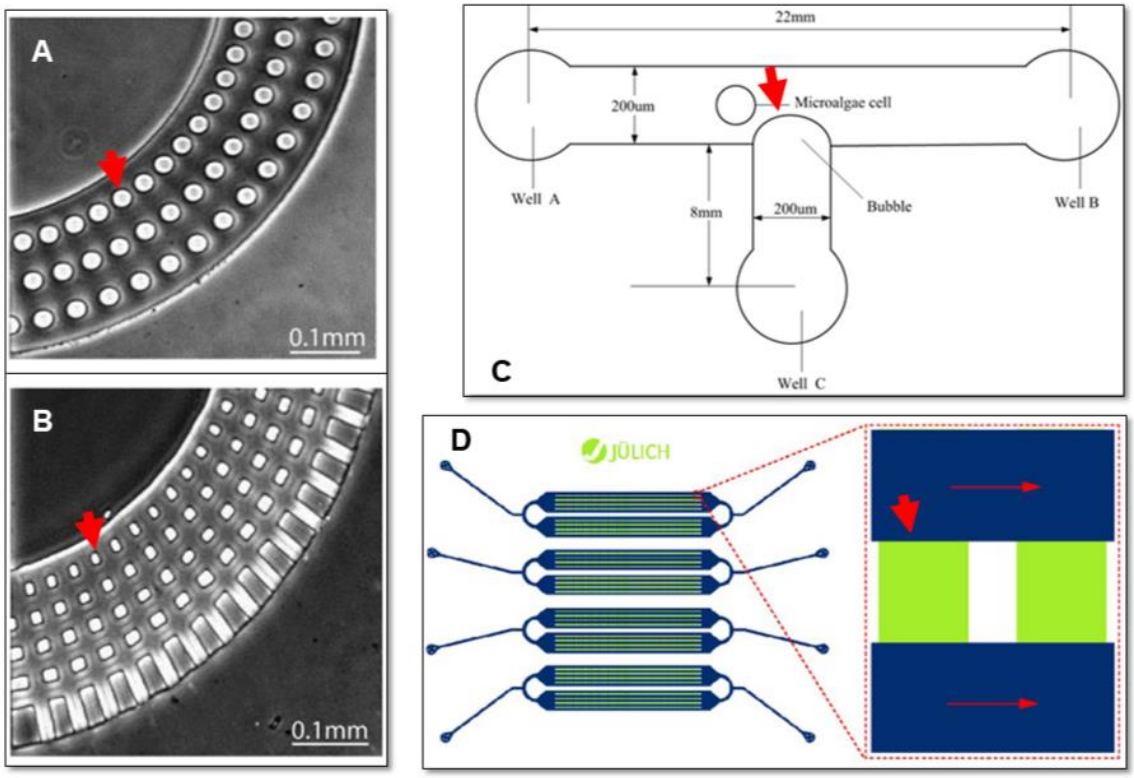

Figure 7. *Different microfluidic devices used to study microalgae at the single-cell level. Thick red arrows indicate trapping areas within the devices. All four devices have been manufactured in PDMS and bonded to glass slides for further observation under the microscope.* **A, B***: devices created by Luke* et al.*, 2016.* ***A*** *was designed to trap* Synechocystis *(±1.75 µm) whilst* ***B*** *was created to grow* Synechococcus elongatus *(0.8-1.5 µm).* **C:** *Technical characteristics of the device designed by Wang* et al.*, 2016. In this case, the cell is captured by an air bubble. Specimens used:* Dunaliella salina *(2.8-40 µm) and* Tetraselmis Chui *(10-14 µm).* **D:** *Microfluidic device created by Westerwalbesloh* et al.*, 2019. Green areas are the chambers where the microalgae was inserted and imaged to follow their growth. Specimen used:* Chlorella sorokiniana *(±3.5 µm).*

The last and most recent device presented in Fig. 7D was developed by Westerwalbesloh *et al.*, in 2019. They presented a device with similar characteristics to that found in the Classical Mother Machine (See *Section 4: Modern Microfluidics*). They created a microfluidic system capable of growing single cells of microalgae (*Chlorella sorokiniana*) to investigate how these responded to changes in light conditions (**Fig. 7**,

D). They were able to study individual changes which could be extrapolated to understand the heterogeneity of a given species' community, paving the path for further investigations interested in specific environmental cues. The device was, once more, made of PDMS and irreversibly bonded to a glass slide. Their system integrated the microfluidic system to an inverted microscope, provided with an incubation chamber and a camera that allowed for recording time lapses every thirty minutes. In addition, the microscope had installed an illumination unit with LED lights. Medium was completely renewed every 1 minute, avoiding depletion of nutrients which allowed for a normal growth of the cells. Worth noting and relevant to the present project is the fact they accidentally recorded an interaction of *Chlorella sorokiniana* with a parasite. The interaction was not investigated further but showed another potential use of their microfluidic device.

1.7. Project Objectives

Bearing in mind the studies previously reported and in order to study the growth dynamics of *O. tauri*, the present study set the following objectives: (**1**) to analyse the growth of *O. tauri* and their potentially associated bacteria at the population level using spectrophotometry techniques; (**2**) to analyse the biocompatibility of PDMS (former material of the microfluidic devices) with *O. tauri* and; (**3**) to test the feasibility of three different microfluidic devices, named Lagoon-like devices, Mother Machine devices and Modified Mother Machine devices, to grow *O. tauri* at the single-cell level.

2. MATERIAL AND METHODS

2.1. Algal Materials:

2.1.1. Preparation of algal material

Natural sea water (NSW) was obtained from Brixton (Plymouth, UK). NSW was previously filtered by passage through a millipore membrane filter of 0.22 µm size (Sigma-Aldrich) and kept in dark for two months, it was then sterilised by autoclaving for 15 min at 121˚ C. Culturing media (L1, adapted from Guillard and Ryther, 1962) was prepared as specified in the medium kit by the provider (NCMA, *Bigelow*

Laboratory for Ocean Sciences). L1 formulation consisted of the following elements: $NaNO_3$ 1mL/L; $NaH_2PO_4xH_2O$ 1mL/L; Trace elements solution 1mL/L and; vitamins solution 0.5 mL/L. Compounds were added to NSW under the laminar flow hood using sterile 5mL plastic syringes and 0.22 µm Whatman syringe filters and mixed until homogenised. The mixture was then filtered using a filtering station with a 0.2um Whatman pore size glass filter applying vacuum. The filtered medium (L1) was then placed into a 1L Duran bottle previously autoclaved and kept in cold (4˚C) until used. *Ostreococcus tauri* (strain *RPN2*) was maintained in 40 mL tissue culture flasks in a total volume of 20 mL in an incubator under a 12:12 h light regime (light: dark cycle) and a light intensity of 15 µmol/(m^2 ·sec) at 18±1.5˚C. Maintenance of *O. tauri* was accomplished by sub-culturing at a dilution of 1:10 (algal culture: L1 medium) every 7 days. In order to reduce bacterial growth a mixture of antibiotics (AB) were added to the cultures as performed by Grimsley *et al*. (2009) with slight modifications: 0.05 g Ampicillin, 0.01 g Gentamicin, 0.02 g Kanamycin, 0.1 g Neomycin per millilitre of sterilised milliQ water (purchased from Fisher Scientific or Sigma-Aldrich). AB were adjusted to a final concentration of 1:1000 per volume of culture.

2.1.2. Measuring algal and bacterial growth at the population level

In order to determine the exponential phase of *O. tauri*, fluorescence intensity (FI) was measured as Raw Data for (440-15/680-20) nm at a gain of 1500 using a spectrophotometer (ClarioStar, BMG Labtech). Absorbance was recorded as an indirect measurement of the optical density at 600 nm (OD_{600}) data which was also used as a reference of bacterial growth as suggested by Griffiths *et al.*, 2011 . To avoid bias in data collection this procedure was performed in 5 different replicas for 21 sequential days within the timeframe of 10:00 am and 12:00 am.

2.2. Microfluidics

2.2.1. Microfluidic designs

The current study made use of three different microfluidic designs which according to their shape were named as follow: (A) *Lagoon-like* devices (B) Modified-*Mother*

Machine devices and (C) *Mother Machine* devices. Graphical abstract of their design can be observed in **Fig. 8**.

The devices were divided in areas according to the camera frame to ease the process. In this way, each of the images contains one single individual area, which in turn contains approximately 20 individual arms. Then the areas with the highest number of algae trapped within the arms was randomly selected to further analyse. The images were analysed using ImageJ and, the bacterial and algal cells were manually counted.

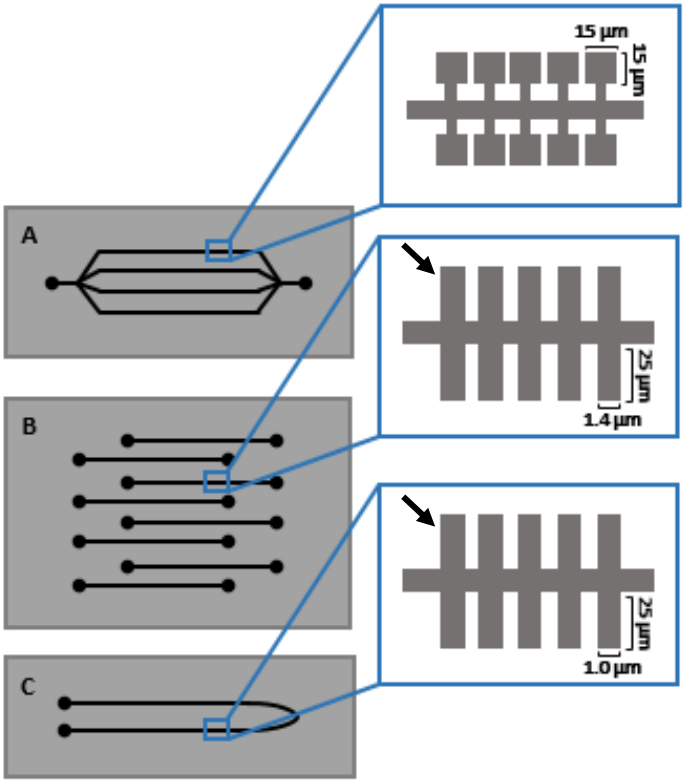

Figure 8*. Different microfluidic designs used.* ***A****:* **Lagoon-like device**, *composed of 4 main channels equipped with 30 pairs of lagoons respectively (240 throughout the chip). Depth of lagoons is 15 µm.* ***B****:* **Modified-Mother Machine *device***, *comprising of 8 independent designs, differentiated by the width of the arms (black arrow). Briefly, each independent device consist of one main channel through which fluid is administered throughout the arms.* ***C****:* **Classical Mother Machine *device***: *internal structure is similar to that found in B. External pattern distribution of arms (black arrows) and inlets and outlets are slightly different as observed. In addition, arms in* ***C*** *are narrower than in* ***B****. Depth in* ***B*** *and* ***C*** *is 1 µm Black dots on the extreme refer to inlets and outlets respectively.*

2.2.2. Fabrication of microfluidic devices

Of all three devices, only the *Lagoon-like* chip was designed and created specifically for this project by Jari Iannucci. The latter was created in AutoCAD and consisted of respectively, an inlet and an outlet orifices, which in turn, were connected to a linear channel that diffused into four different channels. These 4 channels were subdivided into pairs in line with their width sizes, 2 exteriors and 2 interiors. Along all four channels, the squared chambers were positioned as shown in **Figure 8**, containing 60 per linear channel and a total of 240 throughout the chip. All chambers had the same volume.

Fabrication of *Lagoon-like* device silica moulds made use of the clean-room equipment and involved the following procedures: 1) Cleaning the silicon wafer. 1a) Silicon substrate was cut in 2 pieces which were then cleaned with acetone and isopropanol using ultrasonic agitation for 5 min at 25 ˚C; 1b) Cleaned pieces were soft baked for 10 min at 200 ˚C; 2) Deposition of Photoresist on silicon wafer. 2a) the resultant silicon substrate pieces were then placed in the spin coater and casted upon it (SU-8 photoresist MicroChem Corporation); 2b) 2 different spinning steps were applied in the spin coater: first, at 500 rpm, 500 rpm/s for 5s and, secondly at 6000 rpm, 1000 rpm/s for 30s. 3) Soft bake. 3a) Substrates were pre-baked for 10 min at 65˚C. 4) UV-Exposure and Post-exposure bake. 4a) Substrate-photoresist masks were exposed to UV light using a mask aligner (exposure cycle 1 s, hard contact 5 s, exposure time 1.8 s) and post baked (1 min 65 ^{o}C, 5 min 95 ^{o}C); 5) Developer. 5a) Degraded photoresist-masks was removed and replaced by placing it in the oven filled with the developer which was manually stirred occasionally for 30s. 5b) once structure was visible on the surface, the filling was flushed away with nitrogen and checked under the microscope. 5c) when the microfluidic structure appeared clear and clean upon the silicon substrate, isopropanol was applied to stop the action of the developer. This latter step was repeated until completely clear, stage in which the resultant mask was washed with MiliQ water in order to thoroughly remove any remainder of the developer. 6) Hard Bake. 6a) Hard-bake of the masks were performed twice, first at 65^{o}C for 1 min and later for 1 min at 95^{o}C.

Mother Machine and *modified Mother Machine* designs were epoxy moulds (see Estévez-Torres *et al*., 2009, for brief protocol) hence no previous fabrication was needed to prepare the PDMS final microfluidic devices. Epoxy Mother Machine device mould was given to us by Prof. S. Jun; epoxy mould of the Modified Mother Machine was provided by Dr. T. Bergmiller.

2.2.3. PDMS Devices Preparation

The preparation of devices was realized by mixing poly-dimethyl-siloxane (PDMS, SylgardTM 184) at 1:10 (curing agent: base). The mixture was then poured onto the moulds and cured for 60 minutes at 70˚C in an oven. The PDMS was peeled off of the silica/epoxy mould with a scalpel and cut into independent devices using a razor. Inlets and outlets were created with a 0.75 mm biopsy puncher (Harris Uni-Core, WPI). PDMS chips were irreversibly bound on a thin cover glass as stated in Bamford *et al.,* 2017. Briefly, both PDMS and glass slide surfaces were exposed to oxygen plasma treatment for 10 s exposure to 30W plasma power (Plasma-Surface-Technology, Diener electronic GmbH + Co. KG). Such exposed surfaces were manually put into contact, in order to ensure the proper binding between surfaces, extra pressure was applied using the back side of a tweezer on the already sealed device. Tubes used to provide constant flow to the system through inlets and outlets had a dimension of ID=0.38 mm and OD=1.09 mm (Fine Bone Polythene, PORTEX™, Smiths Medical International, Ltd.). Steady supply of media was achieved by connecting inlet tube to a 20 mL syringes (BD plastic) with a 25G needle (Microlance Hypodermic, BD) and incorporated to a portable pump (Model Fusion 200, Chemix Inc.) that allowed to set a precise and controlled flow rate according to needs.

2.3. Experimental:

2.3.1. Microalgae-microfluidic experiments

Lagoon-like devices were tested positively to grow *O. tauri* at a single-cell level when using a diluted sample. Two serial dilutions were performed to achieve a 1:100 dilution. Microalgae clumps were found at the bottom of the flask. From this area, 100

µL were pipetted in a 1 mL Eppendorf along with 900 µL of fresh media. These aliquots were shaken throughout before loading into the devices.

When using the Modified/Mother Machine devices, if interested at a single-cell information, a high concentration of cells in liquid samples is required to accomplish a high quality image level (Bamford *et al.*, 2017).. In order to obtain high concentrated aliquots, initial 20 mL sample bulks were divided into two 50 mL Falcon tubes and centrifuged at 6500xG at 18˚C for 7.5 min. Supernatant was then transferred into two new 50 mL Falcon tubes and centrifuged up to three times under the same conditions. In between centrifugations, pellets were collected and mixed simultaneously by gently pipetting throughout in a unique 1.5 mL Eppendorf tube. After this process, sample was reduced to a total volume of ca. 1 mL of concentrated microalgae. Subsequently, a 1 mL sterile plastic syringe (BD Plastipak™) was loaded with approximately 0.5 mL of the specified concentrated sample. A sterile 25 G needle (BD Microlance 3™) was used to transfer the sample into a fine polythene tubes (ID=0.38mm/OD=1.09 mm, Fine Bone Polythene, PORTEX™, Smiths Medical International, Ltd.). Microfluidic devices were filled with the concentrated microalgae by fitting the latter tube directly into the microfluidic inlet.

In order to maximise the sterile conditions of the system, microfluidic devices were rinsed with 100% ETOH, dried out with pressurised N_2 (g) and left over night in a Petri dish sealed with Parafilm until used. In addition, in the experiment day, microfluidic devices, syringes, needles and tubes were exposed to UV light under the laminar flow hood for 30 min right before binding them irreversibly to the glass-slide.

Steady supply of media was achieved by connecting inlet tube to a 20 mL syringes (BD plastic) with a 25 G needle (Microlance Hypodermic, BD) and incorporated to a portable pump (Model Fusion 200, Chemix Inc.). Once the sample was loaded, the media was pumped at 500 µL /h to wash the main channels. Then, flow rate was set to 100 µL /h for the rest of the duration of the experiment, unless otherwise stated.

2.3.2. Biocompatibility of microfluidic devices

Considering FI and OD_{600} as main indicators of the state of the cultures of *O. tauri*, potential effects of PDMS on microalgae were analysed by recording the variations in such parameters for 22 consecutive days using a photochlorometer (ClarioStar, BMG Labtech). The procedure followed to measure FI and OD_{600} was identical to that explained in *section 2*. In this case, to test the potential effects of PDMS on *O. tauri* three different culture flasks of 20 mL were established: i) Control: 1:10 diluted *O. tauri* culture; ii) PDMS ETOH: 1:10 diluted *O. tauri* culture with a cured PDMS cube (2 cm^3) which had been previously sterilised with 100% ethanol and dry out with N_2 (g); iii) PDMS Autoclaved: 1:10 diluted *O. tauri* culture with a cured PDMS cube (2 cm^3) which had been previously sterilised by autoclaving.

2.4 Image Acquisition and Statistical Analyses:

Microalgae-loaded microfluidic devices were observed under an epifluorescence inverted microscope (IX73, Olympus) using x100 oil immersion objective and images were acquired with a sCMOS camera (Zyla, Andor) using Solis Software (Andor Technology, Oxford Instruments). Experiments were prolonged up to 7 days (otherwise stated when different), for the duration of the experiment, images were taken on daily basis between 10:00-12:00 am. Portable pump supplying media to the Microalgae-microfluidic system was manually disconnected from energy and transported to the microscope facility. In order to corroborate the presence of algal material, images consisted in a set of bright field (direct algal observation) and fluorescence (chlorophyll autofluoresence) (FITC-TRITC filter/475-490 nm; 540-565 nm).

Images were manually analysed using ImageJ (Fiji processing package, Schindelin *et al*., 2012). For the interpretation of the images taken, bright field and fluorescence images were both taken in consideration, independently or jointly, depending on the objective analysed for each variable. For the current study, variables were: growth, when an increase in the number of cells was observed; latency, when the number of cells (*O. tauri* and bacterial included) remained the same; death, when a decrease in the number of cells occurred; and ratio bacteria/ algae.

Statistical analyses were performed using GraphPad Prism version 9.00 for Windows.

3. RESULTS

3.1. Algal and Bacterial Growth at the Population Level

In order to determine the growth curve of *O. tauri*, fluorescence intensity (FI) at 680 nm was measured using a spectrophotometer. Bacterial growth has traditionally been measured by the absorbance at 600 nm, also called OD_{600} (Griffiths *et al.*, 2011), however, since our cultures were not axenic, OD_{600} was instead used to have an estimation of the combined biomass of bacteria and algae. Measurements were carried out for 5 different cultures of *O. tauri* as shown in **Figure 9 (A)**. As observed in the graphs, different growth phases of *O.tauri* were assessed. For the fluorescence intensity (A), there exists a latency or lag period (a) until day 7 where the exponential phase (b) of the cultures starts and lasts for 7-9 days, time after which the stationary phase (c) is illustrated by the steady measurements of the fluorescence from day 16 on. After day 20, cells start to show a decrease in fluorescence indicating the death phase (d).

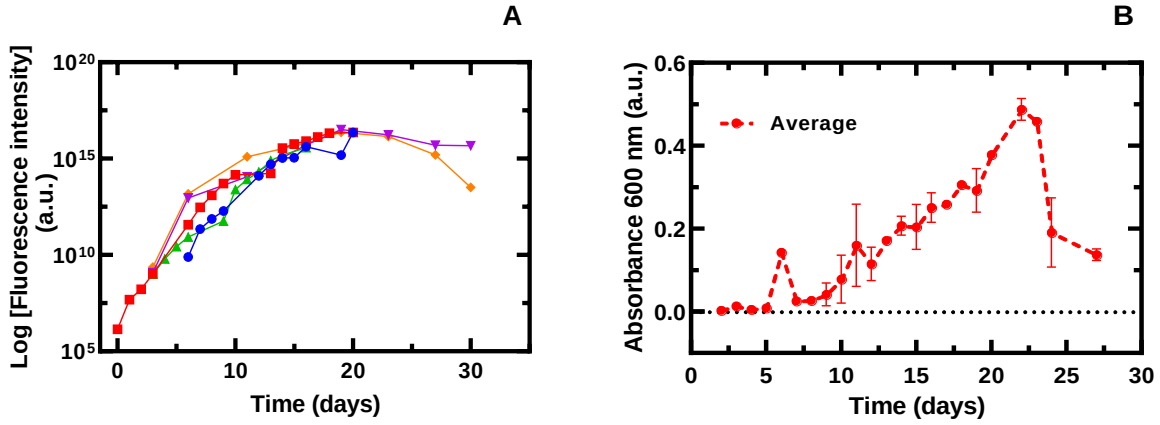

Figure 9. *Normalized values of the fluorescence intensities for different replicas and average with SD Error bars of the raw data of OD_{600} for* O. tauri*. At t= 7d,* O. tauri *starts its exponential phase which is followed by a linear phase for 5 days, after which the stationary phase starts. Death phase, (t= 23d) is confirmed by the drop in FI as algae died. Graph **B** shows the absorbance at 600 nm (OD_{600}), also in absorbance units. Variability within OD_{600} seems to be smaller implying a steadier proliferation of bacteria.*

The growth of bacteria, as indicated in *Material and Methods*, can be estimated in a liquid sample by the fluctuations in the values of the absorbance at a wavelength of 600 nm (Griffiths *et al.*, 2011). The curve for OD_{600} follows the same trend than that found with FI, indicating that bacteria grow at the same pace than *O. tauri*. These data could potentially be indicating the presence of bacteria and it would reinforce the idea of mutual need (algae on bacteria) to survive (Abby *et al.*, 2014).As mentioned in Section 2.3.1 (*Material and Methods, Experimental*), a high concentration of cells was desirable for setting our microfluidic-imaging system, hence cultures at the exponential stage were chosen for the experiments.

3.2. Biocompatibility of microfluidic devices

Up to date, there are reports showing the compatibility and feasibility of the use of PDMS-based microfluidic devices for culturing algae (Bodénès et al., 2019). Similarly, in this study, we set out to confirm that PDMS does not impede algal growth. To do so, three different *O. tauri* cultures were treated as follows: (i) Control: *O. tauri* culture; ii) PDMS ETOH: *O. tauri* culture with a solid PDMS cube (2 cm3) which had been previously sterilised with 100% ethanol and dry out with N2 (g) and; iii) PDMS Autoclaved: *O. tauri* culture with a solid PDMS cube (2 cm3) which had been previously sterilised by autoclaving.

Similarly to the previous section, growth of *O. tauri* is represented by the FI curve in **Fig. 10**. According to the graphs, there were no significant differences found between treatments for the FI as observed by the steady growth showed by the three different treatments. Bacterial growth was estimated by the growth on OD_{600}, all three treatments presented a similar growth pattern. The results suggested that bacteria grew in the same way than without the presence of PDMS, hence the biocompatibility of the PDMS devices.

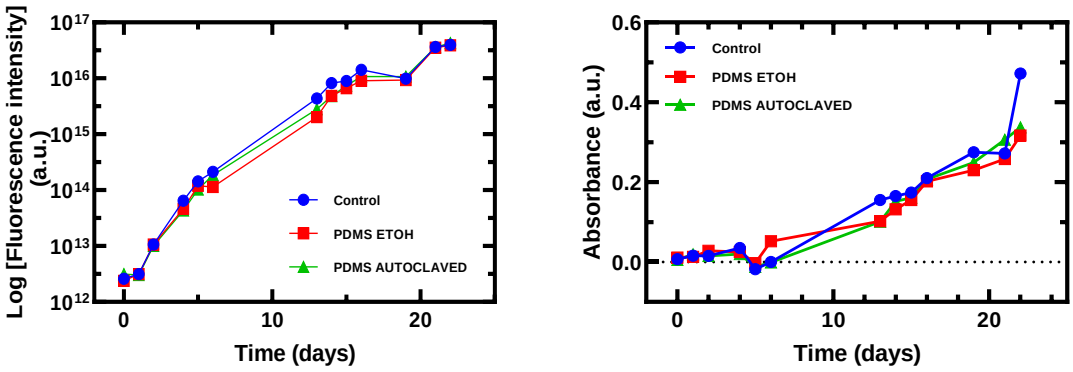

Figure 10. *PDMS effects on* O. tauri *growth. Normalised Fluorescence intensity values showed no significant differences between treatments. Similarly, no differences between treatments were found for* OD_{600} *measurements, although Control values are slightly higher than those found in PDMS ETOH and PDMS Autoclaved, showing a marginally bigger presence of bacteria.*

In addition, it has to be highlighted that other investigations have suggested that the achievement of axenic microalgal cultures is a difficult task (Kazamia *et al.*, 2012; Abby *et al.*, 2014). Consequently, to avoid external contamination coming from the PDMS, sterility was also a parameter of interest, and as stated before, proliferation of bacteria (and potentially cell debris from *O. tauri* too) was estimated by the changes observed in the optical density at 600 nm. Thus, feasibility of the microfluidic-microalgae system was corroborated and the best sterilization method for the microfluidic devices was done using 100% ethanol as OD_{600} values were smaller than those presented by the other treatments (black arrow, indicating red line or PDMS ETOH treatment).

3.3. Algal and bacterial growth at the single-cell level: Microfluidics

3.3.1. Algal and bacterial growth in a lagoon-like device

Different studies have shown the viability of microfluidic devices to grow different type of organisms, from yeast to nematodes (Hwang and Lu, 2013; Jo and Qin, 2016).Others have focused on the cultivation of microalgae with biotechnological purposes (Zhang *et*

al., 2020). Such studies mostly focus on the population-level growth since their ultimate objective was to commercialise specific compounds to offer the final product to the global market, and thus to obtain an economic profit (Gouda, 2021).However, the current study shows a novel microfluidic device in which *O. tauri* can grow freely in a controlled environment, potentially avoiding external stressors. As previously mentioned, environmental conditions were controlled using a portable pump that allowed us to supply the microfluidic device with fresh media at a constant rate of 1 µL per minute. The initial target was to seed a single cell of *O. tauri* in each lagoon-like device and follow growth through time.

Cell count per unit volume was not a viable method due to the lack of tools for its realization, instead, cell concentrations were estimated by dilution factor. Samples were selected according to their colour (strong green vs light green) and by the growth phase previously known by the measurements of their fluorescence intensity (see *Section 3.1.*). First experiments were done using a 1:10 dilution which accomplished an average of ca. 10-15 cells/lagoon at t=0 (**Fig.11**). Next, a dilution of 1:100 was chosen, this resulting in an initial density between 1 to 5 cells/lagoon (**Fig.12**).

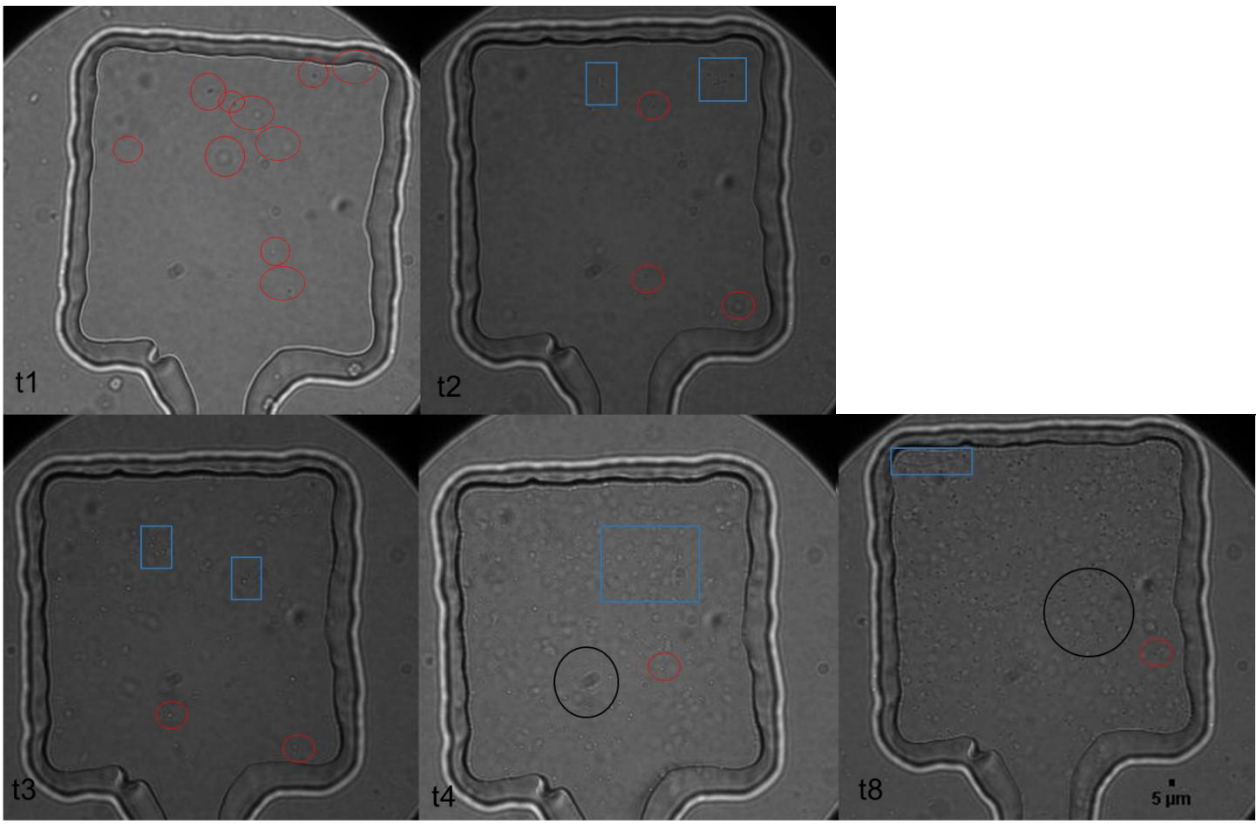

Figure 11. *This composition tracks a microfluidic chamber within the Lagoon-like device. In this case, the dilution used was 1:10, hence the initial number of cells is approximately 10 (**red circles**, algae). This experiment lasted for 8 days (**t8**), and was imaged every day. Bacteria can also be observed (**t2**, **t3**, **t4**, **t8**, **blue squares**), these increased in number with time. The discrimination between algae and bacteria is difficult, as cells look similar, see for example, t3. As discussed above, movement of the cells is noticeable (**t4**, **t8**, **black circles**). Such movement is caused by the 3D available space, which at the same time, also affects the quality of the images: zoom had to be applied to different layers of the samples in order to capture all the living forms present. This phenomenon is also observable as marked by the light green circle in day 7 (G). As expected this effect worsen over time and with the corresponding increase in the number of cells.*

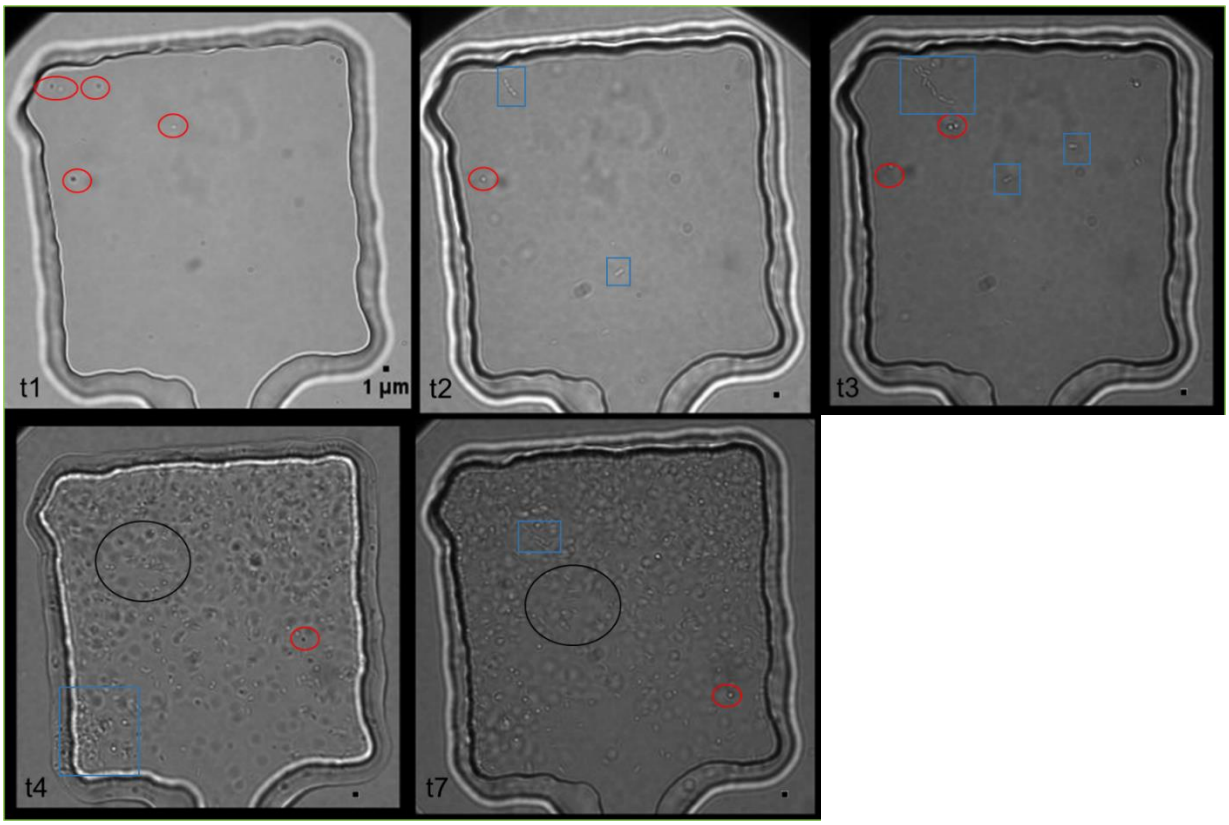

Figure 12. *Lagoon-like device imaged under an x100 magnification objective. The proliferation of O. tauri (**red circles**) and associated bacteria (**blue squares**) can be observed. Initial algal concentration was 1:100, so initial number of algal cells was approximately 5 (**t1**). In **t2** days, algae are hard to localize whilst the emergence of bacteria is noticeable. In **t=3**, what appears to be an algal cell has doubled. In this same day, it can be observed the apparition of a chain of 4 cells of bacteria. Proliferation of such a chain can be followed until **t4**, where bacteria has already grown to up to 10 cells. After day 4 (e.g., **t7**), and as previously explained, drawing a distinction between the types of cells observed is difficult, amongst others, because of the movement of the cells (**black circles**).*

1:10 dilution shows a consistent and steady growth, whilst in 1:100 experiments are more heterogeneous as showed by the standard deviation (**Figure 13**). Heterogeneity that was interpreted through the fluctuations in the standard error in the 1:100 dilution was understood as different cell behaviours (e.g., latency, death or growth). Such

changes are thought to happen in response to the intraspecific variability between individual cells within a given population (Kremp *et al.*, 2012).

As observed in the graphs, *O. tauri* showed an apparent rapid growth, but after 3 days of experiment, the determination the exact number of algal cells became an arduous exercise due to the rise of bacteria (**Fig. 11**, **12**; red circles for algae, and blue squares for bacteria).

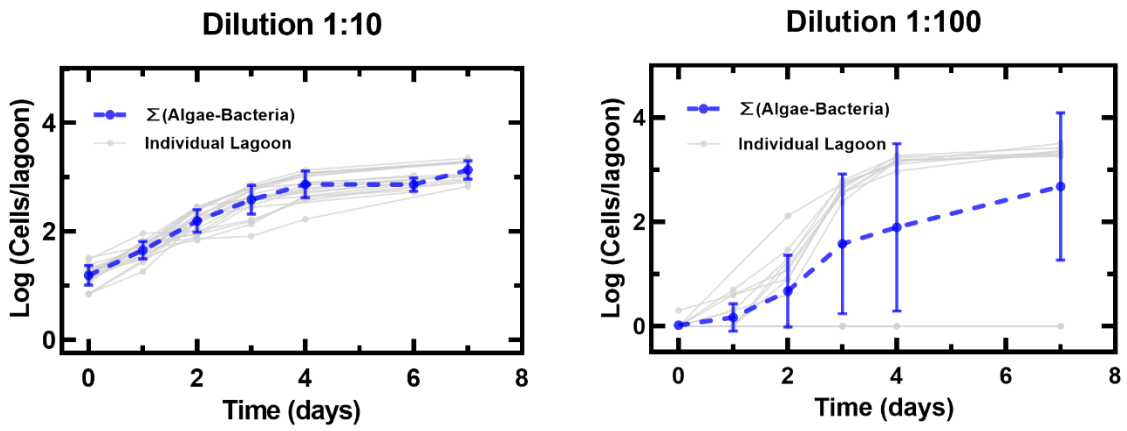

Figure 13. O. tauri *and associated bacteria growth within the Lagoon-like devices. Grey lines refer to the growth per lagoon in contrast with the blue line, showing the mean average of the logarithmic values. Although AB were applied to the cultures, no differences in growth rhythm were found between AB-treated and non AB-treated samples. Other factors that enhanced the difficulty of counting O. tauri cells were the big dimensions of the lagoon-like devices. The contrast between the 1 um of an algal cell against the depth of 15 um, along with the flow of the media through the microchip, allowed the free movement of the cells, making it complex to distinguish between algal and bacterial cells. As shown in the supplementary material, a cell was recorded turning on itself, demonstrating that what initially appeared to be an algal cell, was in turn, a bacteria. This issue was found for both, 1:100 and 1:10, dilution.*

Algae and bacteria were detectable and distinguishable in the first day of the experiments as showed in **Fig. 12** (t1, t2, red circles: algae) and **Fig. 12** (t1, t2, blue squares: bacteria). However, it was not possible to distinguish between algae and bacteria at later time

points, therefore it was decided to count the number of algae and bacteria as a unique entity composed of the summation of both without discriminating between cell types. Autofluorescence was also recorded but it was no avail, since cells were turning around and moving through the lagoons, giving not enough information as to clearly distinguish between cell types. Autoflourescence imaging requires a dark environment and the cells to be still in order to be imaged. If these requirements are not fulfilled, the cells that are being imaged appear blurred, thus affecting autofluorescence measurements.

3.3.2 Algal and bacterial growth in the Mother Machine device

The so-called Mother Machine device has commonly been applied to bacteria to study antibiotic resistance (Bamford *et al.*, 2017; L. Yang *et al.*, 2018; Łapińska *et al.*, 2019; Zhang *et al.*, 2020). One of the limiting factors of such approach is the size of the cross-section of the lateral channels (also called arms, see Section *2.2.1. Microfluidic Designs*) where the cells are hosted, hardly applicable to organisms bigger than 1 um. However, other living forms apart from bacteria, as for instance, *O. tauri*, cells also show a rather small size that makes them suitable to be studied using the above device. In this study, we, for the first time, attempted to culture phytoplanktonic organisms using the Mother Machine device. For this device, no dilution was needed. Instead, and as stated in Section 2.3.1 (*Microalgae-microfluidic experiments*), concentration of the samples was carried out through centrifugation.

The fast spreading of bacteria stunted the growth of *O. tauri* by taking over the physical space, resulting in the microalga dying. **Figures 14** and **15**, shows the growth of *O.tauri* and bacteria within the Mother Machine device in day 0 and 3, respectively. Thereby, although *O. tauri* was able to grow, success in reproducing its growth again was not accomplished and, therefore, we believe that this device cannot be used to grow non-axenic microalgae.

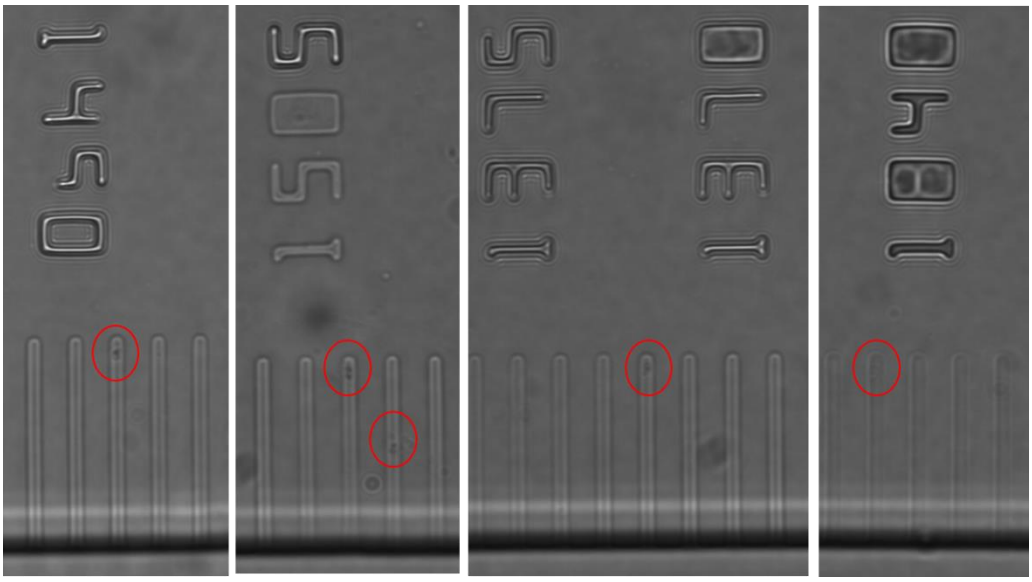

Figure 14. *Different algal shapes found throughout the duration of the experiment* ***(red circles****). Such behaviours explain the necessity of a complementary approach, such as the auto-fluorescence, to study the growth of O. tauri.*

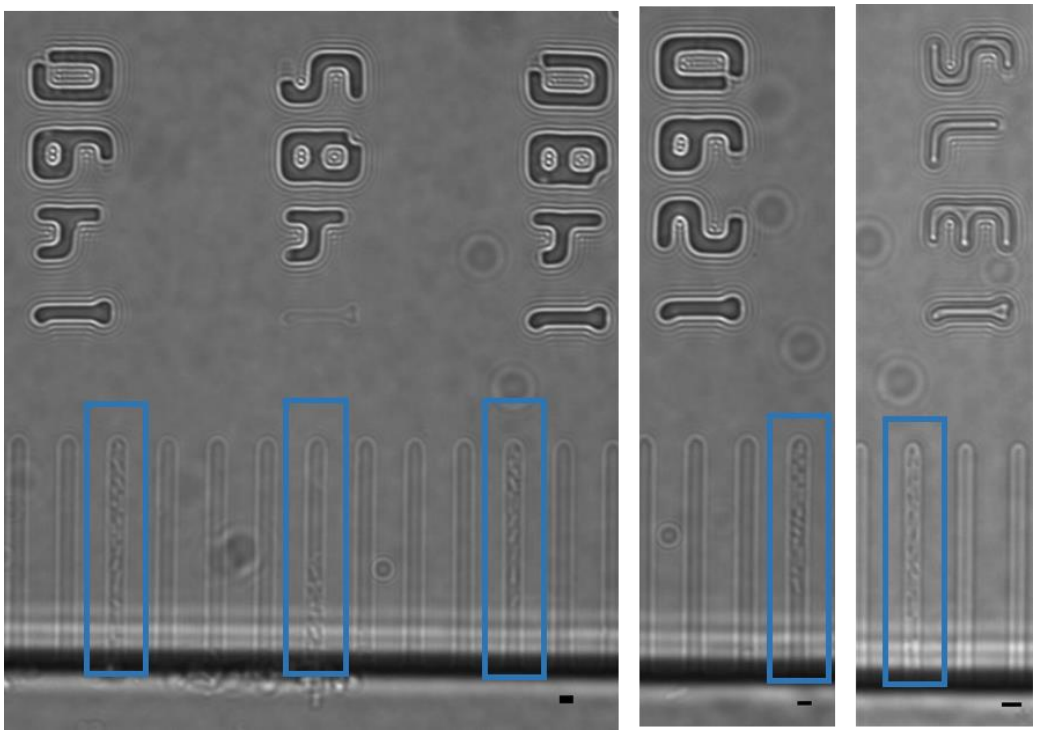

Figure 15*. Mother Machine arms hosting bacteria naturally growing with* O. tauri*. Bacteria are monopolizing the space (**blue quadrangles**), resulting in a lack of space for any other organisms to grow. This proliferation also affected the counting of the cells since shapes are not well-defined, being hard to accurately count them. Scale bars: 1 um.*

Nonetheless, our results showed that in the mother machine bacteria grew similarly to in the Lagoon-like device (**Fig. 16** and **17**).

The rapid growth of bacteria observed in the Mother Machine could potentially reinforce the idea already set by other authors pointing out that the presence of bacteria along with algae under laboratory culture conditions, enhances the growth of the latter (Kim *et al.*, 2014; Fuentes *et al.*, 2016).

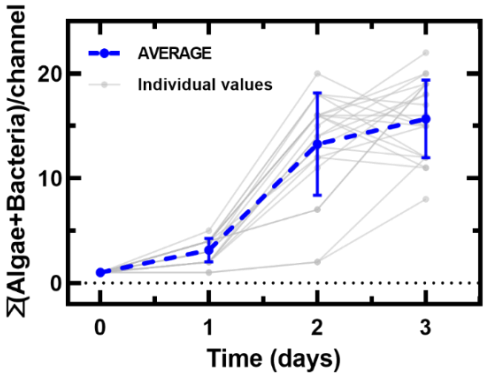

Figure 16. *Algal and bacterial growth using the Classical Mother Machine device (N_f= 22 cells). Y-axis shows the summation of the total of cells, without distinguishing between bacteria and algae.* MM *device is presented as a valid approach to observe the growth of both* O. tauri *and its associated bacteria, yet it is not the most adequate tool to analyse the single-cell growth of* O. tauri*. Bars indicate Standard Deviation.*

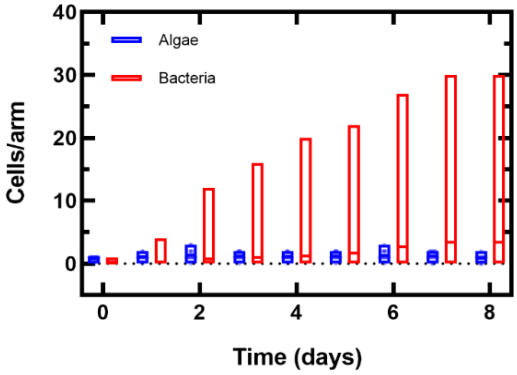

Figure 17. *Growth of bacterial (red) and algal (blue) cells within a Classical Mother Machine device. Exponential growth of bacteria can be observed from t=3 days until t= 8.* O. tauri *shows a reduced growth almost zero. For the current experiment, autofluorescence was recorded in day 7, such fluorescence data is presented in this plot (t=7).*

Fluorescence analysis gave a clearer insight into what it was being observed, as showed in **Fig. 14** and **15**, several oval-shaped cells were not *O. tauri*, or at the very least, cells were not alive and thus auto-fluorescence was not observed. Ral *et al.*, in 2004, pointed out what could be a potential explanation in biological terms for this phenomenon. In the former, formation and division of starch granules was studied for *O. tauri* cells. The current unspecific masses could potentially be explained if they were to be a by-product realised during the growth of *O. tauri*.

3.3.3. Modified Mother Machine devices

As previously described in Material and Methods section, the Modified Mother Machine device consists of 8 independent chips/devices differentiated according to the width of the arms (from 1.0 um to 1.8 um) (**Fig. 18**). Each of the chips/devices had and independent inlet and outlet as shown in **Fig. 8** (see Section *2.2.1. Microfluidic Designs*).

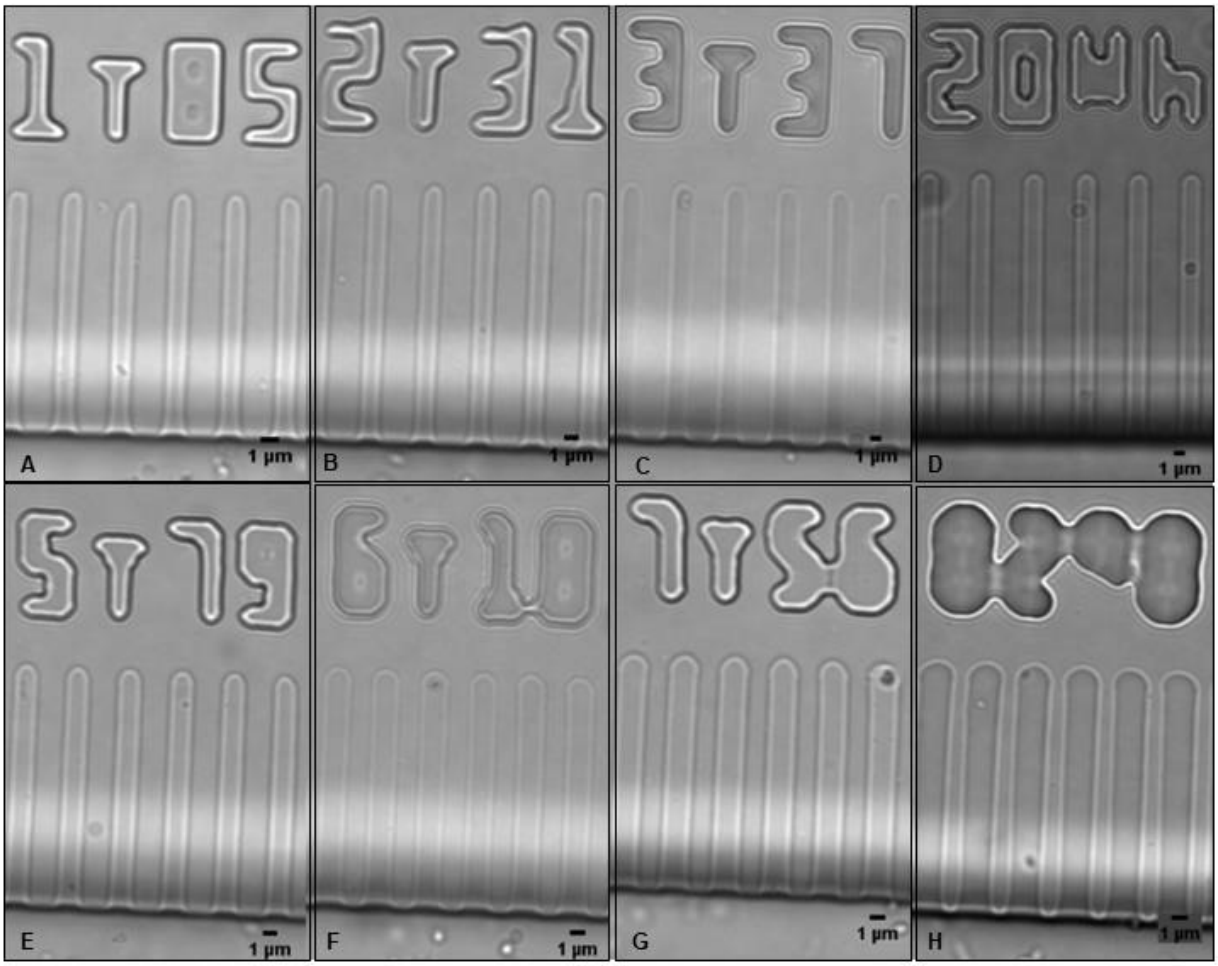

Figure 18. *Different arms within the Modified Mother Machine under the microscope with a magnification of ×100. Width of the arms increase from A to G. As observed bacteria (**A**, **E**) and* Ostreococcus tauri *(**C**, **D**, **F**, **G**). It is noticeable the presence of certain forms that could be by-products or either bacteria or algae in early stages of development (**B**, **H**). All images were taken at t=0 immediately after seeding the device.*

For the present study, all of them were tested in order to determine the most suitable for *O. tauri* cells. The loading of the sample procedure was similar to that for the Classical Mother Machine device. After testing 8 of the arms, we decided to conduct the experiments using the chip number 4 with an arm width of 1.4 um as it showed the highest cell trapping rate. For this device, the growth of *O. tauri* and bacteria was calculated as well as the ratio bacteria/ algae. Since the space within this device available for the algae to grow was bigger, experiments were extended in some cases to up to 10-14 days.

The duration of the experiments differs, as well as the number of divisions, latency events and deaths. There can also be seen unspecific circular shapes which could be a by-product realised during the development of *O. tauri* cells. Ral *et al.*, in 2004 presented micrographs of *O. tauri* cells undergoing division. In them, it can be observed how the cells grew in volume. This result can be compared with the images here exposed (**Fig**. **19**-**21**).

The most prevalent change observed was, as mentioned, the fattening of the cells (**Fig. 20**), which was often followed by the elongation of such cells (**Fig. 21**). Such elongation did not always lead to the subsequent division of the cell, but instead, cells often suffered degradation in size (**Fig. 19**, marker 8, **10** and **24**) (*See Appendix for more images*).

Please note that to facilitate the reading as well as the processing of the data and the images, the experiments were numbered and labelled accordingly, but at no time does this enumeration interfere with the description of the experiments, that is, the experiment number is not a characterization of this at all.

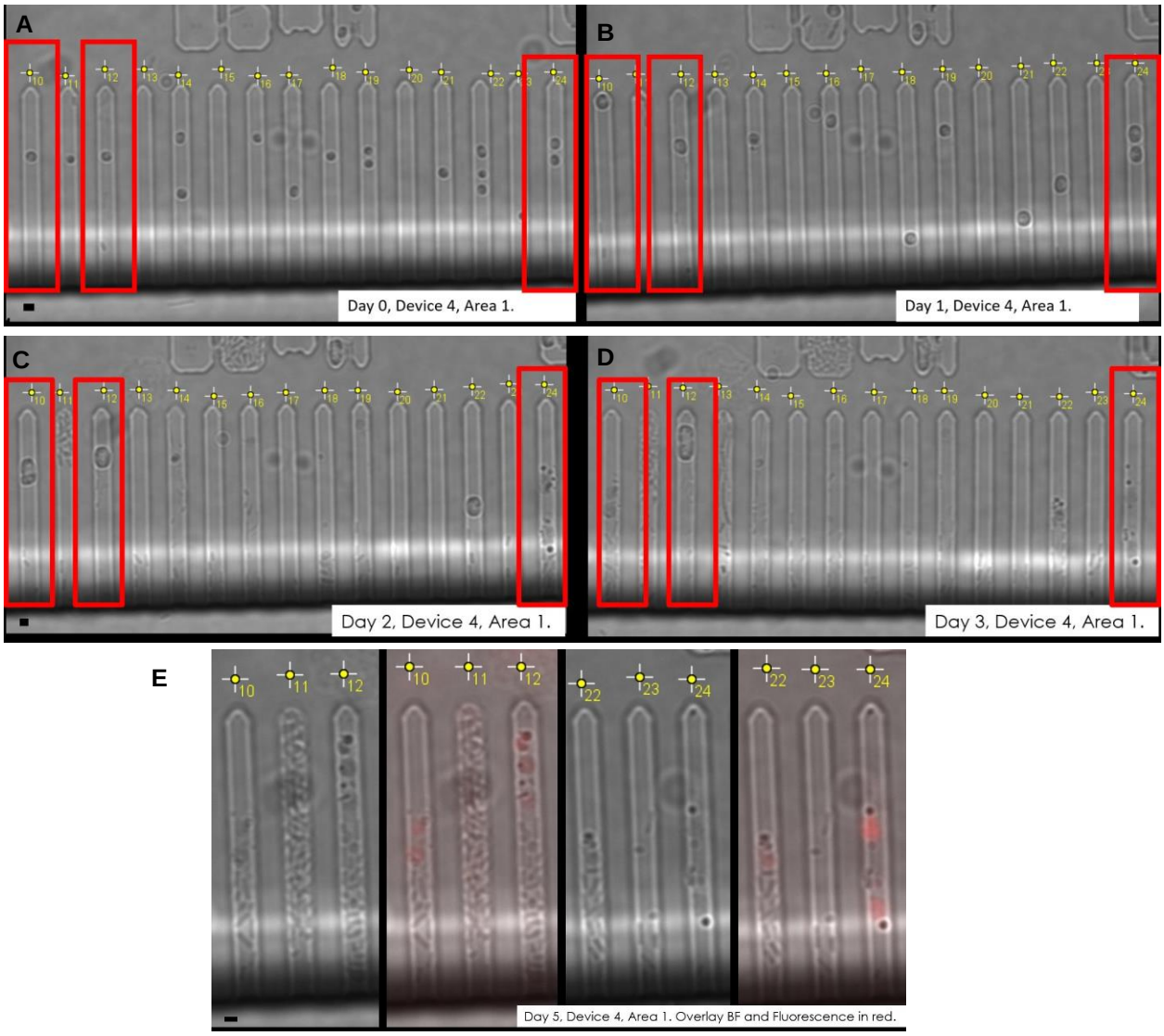

Figure 19. *Development of* O. tauri *within the Modified Mother Machine device 4. Area 1. Yellow numbers are markers. Scale bars are 1 μm. As observed, the initial number of cells varied from 1 to 3 (t=0,* ***A****). After one day of incubation, certain cells started to get bigger (****B****) and by t= 3 the cells have doubled their sizes (****C****). It is also noticeable the proliferation of bacteria. In t= 4 (****D****), several rounded shapes appear where the algal cells were (markers 10, 24). In t=5 (****E****, in red autofluorescence), two division events have happened in arms no. 10 and 12. The latter a double division, (from 1 to 3 cells). Arm 24 presents circled shapes and surprisingly, the amount of bacteria was less than in the other channels.*

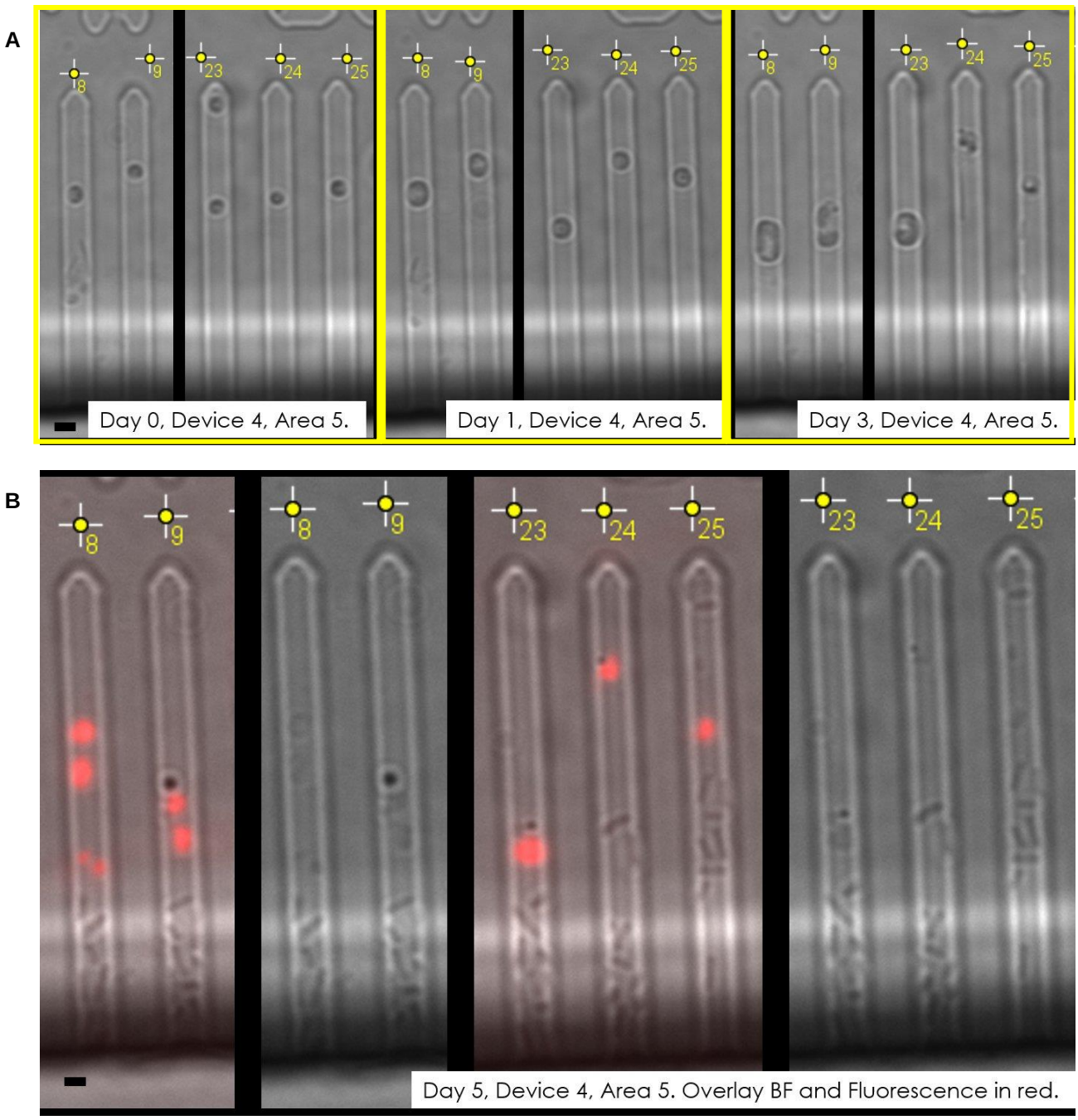

***Figure 20**. Development of* O. tauri *within the Modified Mother Machine device 4. Area 5. Yellow numbers are markers. Scale bars are all 1 μm. For this area, division of* O. tauri *can be observed for the channels 8 and 9 (**B,** in red autofluorescence). For the arms 23, 24 and 25, no division is observed. In day 3 did not present the characteristic elongation which is present in arms 8 and 9. However, the so-mentioned circular shapes appeared, once more, in day 5 (**B**).*

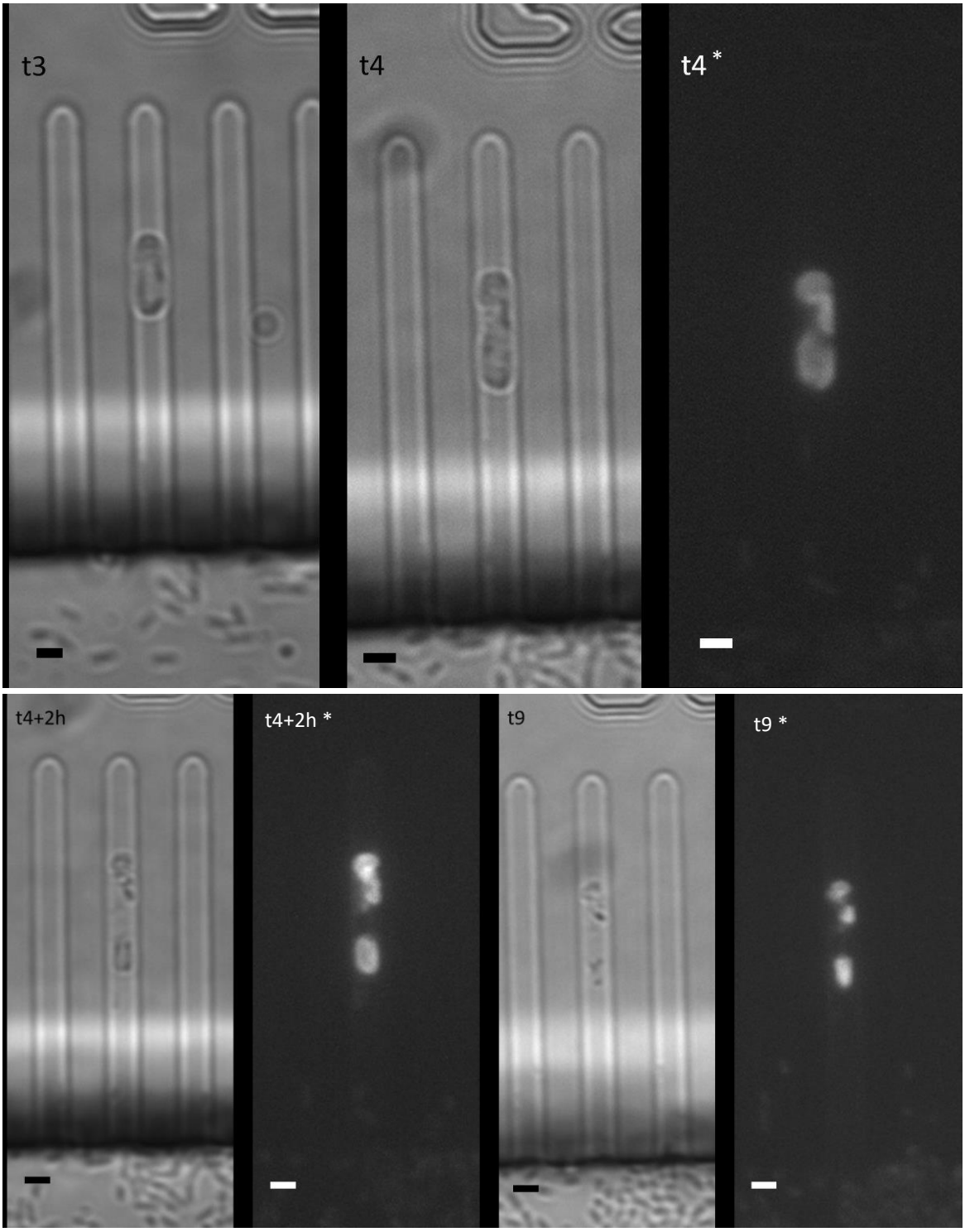

Figure 21. *Development of* O. tauri *within the Modified Mother Machine device 4 (Exp. 20). Scale bars are all 1 μm. Images marked with an asterisk show the autofluorescence. This specific cell was found during the development of the experiment in day 3. Since it had a quite elongated shape, it was followed until the last day of the experiment. However, it cannot be said whether the initial number of cells for this arm was 1.*

Fig. 22 shows the data plotted for two experiments labelled “Exp. 21” (**A**, **B**, **C**) and “Exp. 11” (**D**, **E**, **F**). For experiment 21 the total number of channels analysed was 146 arms (channels); for the experiment 11, N=155 channels. Duration of experiments was of 10 and 7 days respectively. Not surprisingly, the line representing the average value of the ratio is similar to that found in bacterial growth (**Table 1**), due to the small number of algae when compared to that of bacteria. High Standard Deviation could potentially be reflecting the variability within communities, for both algae and bacteria.

Experiment 11 showed a slightly different trend more similar to that found in the experiment 20 (Chips 1 and 2; **Fig. 23**; **Table 1**). For the present, algal growth (**Fig. 22**, **D**) presents a slightly increase by day 3, quickly followed by a decrease in the next days. Contrarily, bacteria (**Fig. 22**, **E**) present an exponential growth from t= 3 days. By the end of the experiment, in day 10, the bacteria took over the channel, not allowing us to count the exact number of cells, hence the lack of SD error bars. The ratio of bacteria per algal cells (**Fig. 22**, **F**), followed the trend of the growth of bacteria alone.

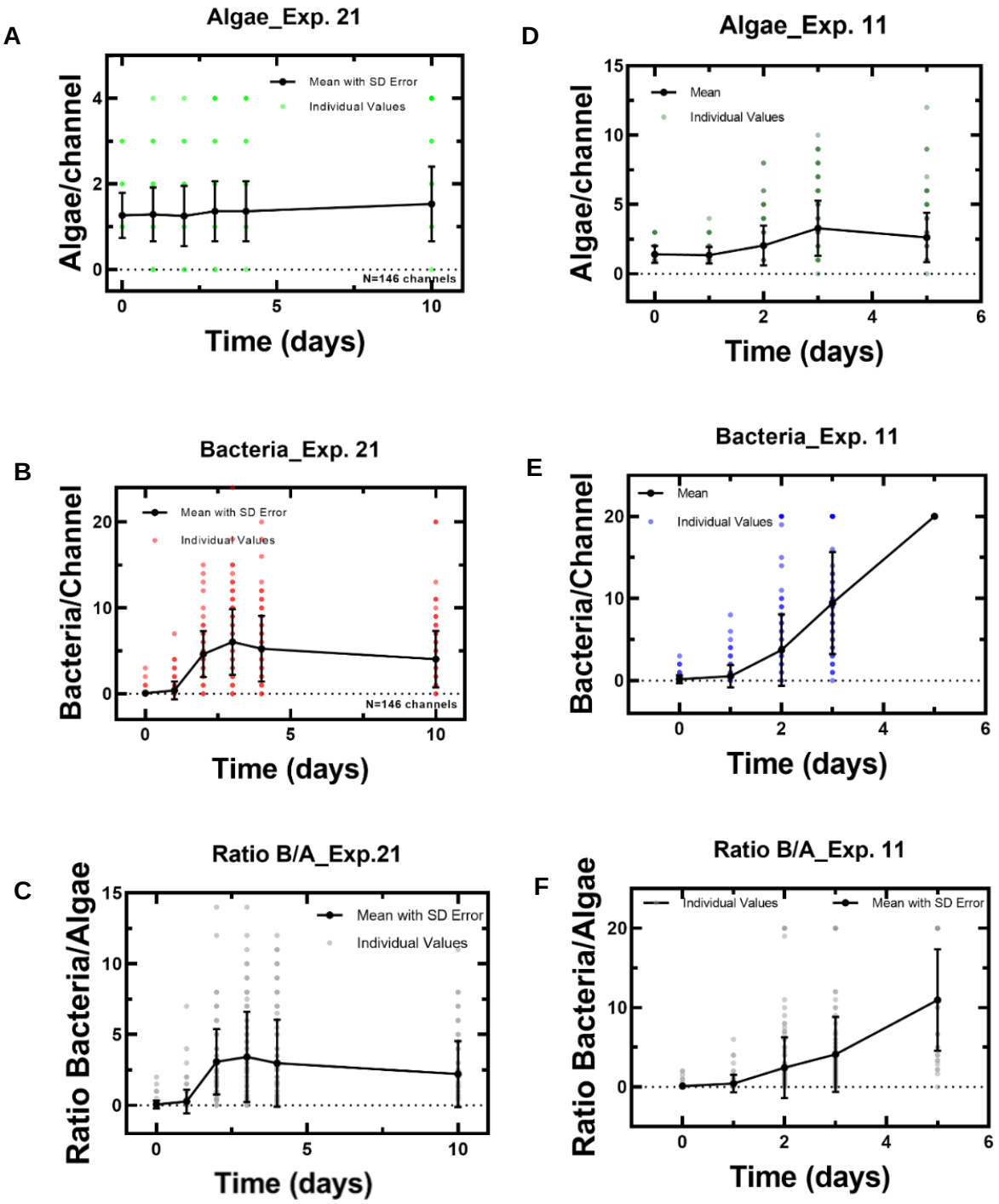

Figure 22. *Growth of algae (**A, D**) and bacteria (**B, E**) and Ratio Bacteria/Algae (**C, F**). Black lines refer to the mean values with the Standard Deviation.*

Coloured dots are individual values, representing number of cells per individual channel. Black lines refer to the mean values with the Standard Deviation. As observed, O. tauri *did not divide (**A**). However, when observing bacterial growth, there is a rapid proliferation after day 3, followed by a slow slight decrease until last day (t= 10) (**B**) in accordance with the data obtained in the lagoon-like and classic mother machine devices. The ratio was calculated for each day of experiment and was calculated dividing the number of bacteria by the number of algae (**C**).*

In **Fig. 23**, the same data is represented for the labelled experiment 20, consisting in two different devices: chip 1 (**A**, **B**, **C**) and chip 2 (**D**, **E**, **F**). For these, total number of channels analysed was of 33 and 74, respectively. For both chips, the duration of the experiments was of 4 days.

Bacterial growth (**Fig. 23**, **B**, **E**), displays, once more, an exponential increase for both chips. However, differences are found in the variability of the data within each experiment: for chip 1, such variability is also reflected in the ratio of bacteria per alga (**Fig. 23**, **C**). Nevertheless, trends for both, chip 1 and chip 2, are similar for all the three variables studied.

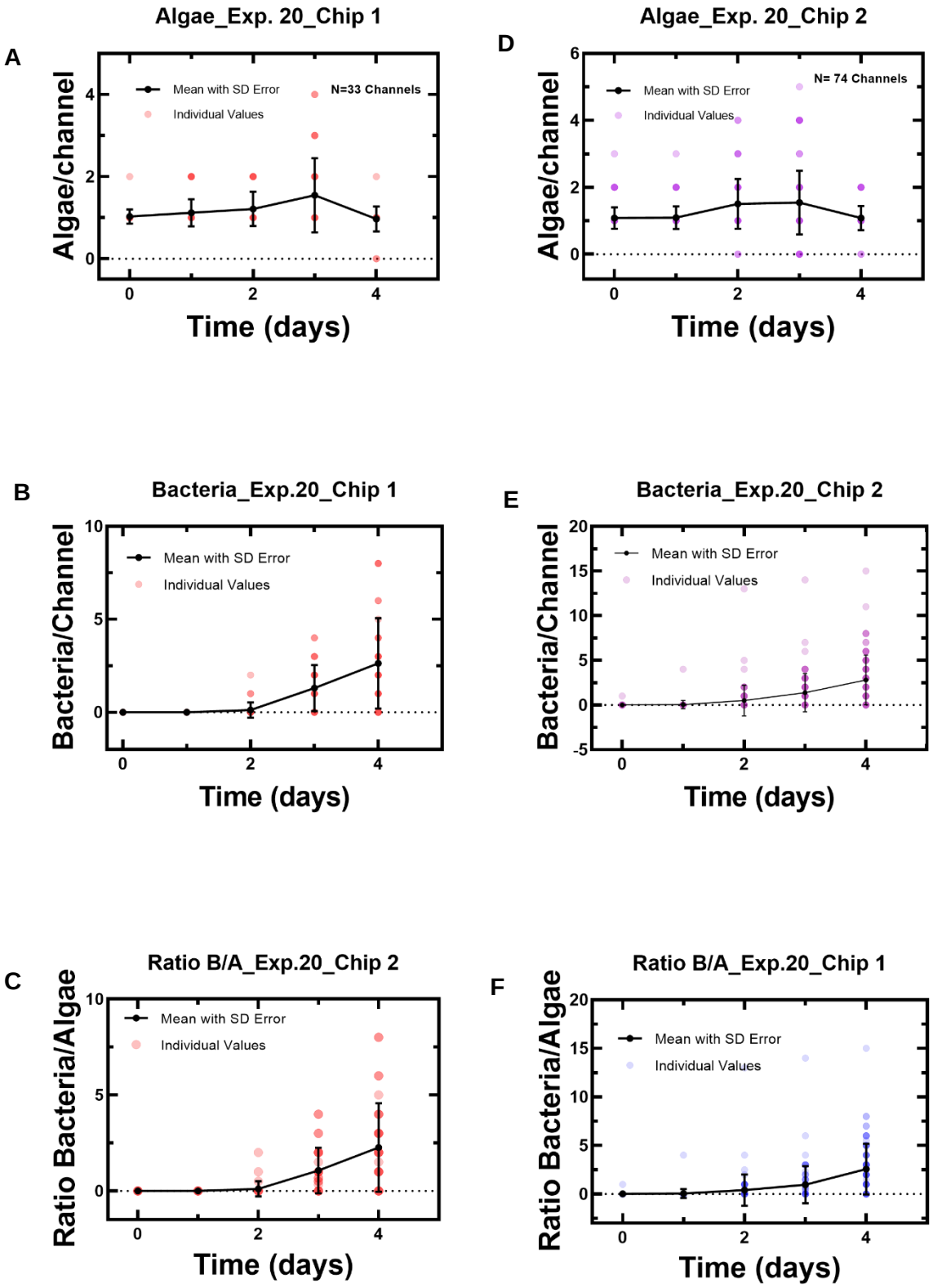

Figure 23. *Growth of algae (**A, D**) and bacteria (**B, E**) and Ratio Bacteria/Algae (**C, F**). Black lines refer to the mean values with the Standard Deviation.*

Coloured dots are individual values, representing number of cells per individual channel. Black lines refer to the mean values with the Standard Deviation. ***A****,* ***B*** *and* ***C*** *refer to chip 1 and* ***D****,* ***E*** *and* ***F*** *are values for chip 2. As observed, trends for both chips are similar. Algal growth (****A****,* ***D****) presents, as in experiment 11, a minimum increase in t= 2 days, which is followed by a decrease, for chip 1 in day 3 and for chip 2 in day 4. Bacterial growth (****B****,* ***E****), displays, once more, an exponential increase for both chips.* ***C*** *and* ***F*** *(ratio bacteria /algae) also present an exponential growth especially determined by the growth of bacteria.*

4. Conclusions, Discussion and Future Perspectives

We developed a microfluidic device capable of tracking cells of *O. tauri* at the single-cell level. The main advantage is that it allows for the long-term following of single cells of the microalgae under a well-controlled physical condition, as for instance: temperature, light irradiance, and medium supply.

Although our objectives were not met with all three devices used in this project, the novel microfluidic designs presented here do represent a step forward for the evaluation of aquatic microscopic samples. We initially investigated three different microfluidic devices to quantitatively analyse the single-cell growth of *O. tauri*. All three devices had different physical confinement characteristics that were visually assessed using an epifluorescence inverted microscope. The Lagoon-like device did not meet our objective of evaluating single cells of *O. tauri*, however, it did allow the track of a larger number of initial cells. Optimization of algal growth within a microfluidic device is a recurrent aim within industry and in this framework, several investigations have developed similar devices to the Lagoon-like presented here (Kim, Devarenne and Han, 2018; Castaldello *et al.*, 2019). The Lagoon-like devices could therefore be applied to analyse different variables that would optimise the growth of a given algal strain in order to maximise its growth for its commercialisation or for the mass production of certain metabolites. However, more experiments should be done to analyse the capability of this specific device to be applied in the marine biology field.

The Classic Mother Machine device allowed us to observe *O. tauri* cells at the single-cell level retaining a high image resolution. Nonetheless it presented a confining

space that was insufficient for *O. tauri* to successfully divide, leading to the early dead of the cells. It has been demonstrated though, that microalgae undergo different physiological changes during their life cycle that affect their size (Frenkel, Vyverman and Pohnert, 2014). We were able to follow the development of *O. tauri* within the arms of this device, which means it has the potential to be a reliable tool to study more specific physiological traits. However, reproducibility of the experiments was not accomplished; it should be analysed further if the cells that were trapped were in a very early stage, thus presenting a smaller size that would have allowed for their capturing within the device. One of the reasons for this lack of reproducibility could be due to the heterogeneity of the algal/bacterial system, where a similar initial condition is hardly achievable.

The Modified Mother Machine device met our goals as in it allowed us to observe *O. tauri* single cells developing, including some divisions too. On the one hand, it allowed for the track of *O. tauri* samples starting from a single cell. On the second hand, images preserved a high resolution which allowed the identification of changes in the microalgal cells that eventually undergone division events as well as those dying or in a latency phase, and lastly, it was reproducible, asserting the feasibility of the device. Why not all the cells divided is an unresolved question. We can hypothesise that the confinement to which the cells were subjected to could have potentially created an adverse environment, and thus the cells cannot reach their optimum size. Another hypothesis could be that when bacteria started growing dramatically, the medium could not diffuse to the end of the channels, meaning that the nutrients in such medium are not reachable by the algae. Another interesting factor that would be worth studying is the already reported fact that algae need the presence of bacteria in order to grow (Abby *et al.*, 2014). If in our devices there were not algae with bacteria in the same arm, algae could not grow, and what is more, it could undergo programmed cell death as reported for other species of algae (Orellana *et al.*, 2013).

This study has proposed, to our knowledge, for the first time, the use of simple microfluidics to investigate *Ostreococcus tauri* at the single-cell level. Up to date, studies using microalgae have made use of integrated systems which are complex to set up (Hong, Song and Shin, 2013; Massalha *et al.*, 2017; Osmekhina *et al.*, 2018).

As observed in several investigations using microfluidics, the arrangement of such systems is complicated as it often needs a combination of knowledge from all different natures (Deng, Guo and Xu, 2020). For instance, the research of new material for its application in microfluidics is an avant-garde field which aims to enable the scientific community to analyse a wider range of variables within a single device; this concerns both, the chemical composition of the material used for the devices, and the materials that are used supplementary to a given microfluidic system (e.g.: lasers, temperature controllers, bubble creation, valves, manifolds, etc.) (Beebe, Mensing and Walker, 2002; Temiz *et al.*, 2015; Kim, Devarenne and Han, 2018). In this project, we minimised the complexity of the system by only using PDMS a cheap and biodegradable material, as the main device material; a portable syringe pump to efficiently supply a continuous medium and an epifluorescence inverted microscope with the capability of recording the auto-fluorescence naturally occurring in algae. This eased the handling and costs of the research. Additionally, it has been pointed out by other authors the challenge of designing devices where the medium supply is continuous and equal in concentration throughout all the trapping spaces of the chip (Castaldello *et al.*, 2019). By using the syringe pumps and because of the design of our microfluidic devices, we present a tool in which this difficulty has been solved.

As already mentioned, our microfluidic system was further optimised using an epifluorescence microscope that allowed us to record and quantify the auto-fluorescence of the algae. Autofluorescence has widely been used to assess the aliveness of microalgal cultures(MacIntyre, Lawrenz and Richardson, 2010; Houliez *et al.*, 2012). The microalgae growth in bulks was determined at the population level using a spectrophotometer whose technology depends on the use of different laser beams, recording the fluorescence and absorbance of the different samples analysed. As showed, it allowed us for the track of the stages of the algae throughout its life cycle making it possible to select samples on the exponential growth to be observed within the microfluidic devices. Along with the estate of the microalgal cultures, we also had an insight into the bacterial presence. Optical density at 600 nm has been traditionally used to detect bacteria (Burmeister and Grünberger, 2020), and by this

method we measured the bacterial growth, which was next visually confirmed using microfluidics, too. Autofluorescence was also used to confirm the state of the cells within the microfluidic devices, as it is a marker for aliveness of microalgae (Bodénès *et al.*, 2019). In this project we recorded differences in the algal shapes (**Fig. 19**-**21**) that no other studies had reported before. Although the number of investigations on the physiology of *O. tauri* are limited, we can correlate our findings with those found by Ral *et al.*, 2004. In this, they imaged *O. tauri* cells undergoing division and followed the development of starch granules. The way of dividing found in their samples is similar to that presented in the present study: first, the fattening of the cells; second, the elongation and finally the division of the cell (Ral *et al.*, 2004). There are also common traits shared amongst groups of the phytoplankton regarding division patterns (Henderson, Gan and Jensen, 2007). This could potentially explain the unspecific masses found in our images. For instance, the dark circles (**Fig. 19**-**21**) could be by-products produced as a response to the physical confinement imposed by the microfluidic channels.

On the other hand, there exists a lack in visualisation approaches on marine ecology at the single cell level. One of the main impediments in these investigations is that the marine environment is complicated to recreate. The application of the present microfluidic system would allow the creation of the different fluid regimes that naturally happen in the aquatic system (e.g.: pycnocline, halocline, turbidity, turbulence, currents). This project did not explore these phenomena but introduces a system which can be modified in order to investigate them. In these terms, a topical issue is climate change whose concern is raising amongst both, Society and the scientific community (Islam and Kieu, 2021). The main consequence of climate change in the marine environment is the increase in the temperature of the oceans which is changing the physic-chemical characteristics of the aqueous systems, hence the importance of creating methodologies that will allow the modification of the fluid conditions in a controlled manner (Sato *et al.*, 2007). Our device could be modified to allow for the study of ecological variables that will be affected by this phenomenon (pH, water temperature, increase of CO2) affecting the phytoplankton group. In this

line, contamination and water pollution are also challenges we face today (Xiao, Liu and Ge, 2021). The pharmacological industry is currently trying to reduce the impact of the by-products generated in both, in the manufacturing process of the drugs and in the management of the wastes of the drugs that are not fully up taken by humans and animals, reaching the oceans (Toutain, Ferran and Bousquet-Mélou, 2010). This industry is investigating new micro-flow through systems and are also incorporating microfluidic devices because they allow for the reduction of the drugs and reagents used (Andar *et al.*, 2019). Microfluidics is also an interesting field for such an industry because it also allows for the use of a precise an accurate concentration of a certain drug and for the in vivo monitoring of the model organism used (Chiu *et al.*, 2017). For these reasons, we believe that the modification of our system could also be a promising tool in this ambit.

Many are the improvements that need to be done in the system here presented, however, the development of the microfluidic devices used in this project pave the path for new investigations. For example, it would be interesting to make changes in the fluid conditions so that new variables con be analysed in both, in the accuracy of the system and in the physiological responses of the organism studied. In this context, the investigation of the physiological changes to environmental fluctuations is also a promising application. *O. tauri* physiological traits haven't been fully studied *in vivo* at the single-cell level (Farinas *et al.*, 2006). To deepen into our findings would be a breakthrough for understanding the population dynamics that often determine the algal blooms and the eutrophication of the water bodies that causes the loss of biodiversity. For instance, the study of this alga under a completely axenic condition, could give us some insights in its dependence or no-dependence of bacteria. Experiments differentiating between algae and bacteria in parallel, and with both organisms together would help us to better understand their specific characteristics as well as the role of each within the phycosphere. Future work should also involve the investigation of the interactions between *O. tauri* and its associated bacteria. Isolation of bacterial cells naturally growing in algal cultures would help in the determination of this interaction as for it has been pointed out by other authors (Abby

et al., 2014; Cooper *et al.*, 2019) the relationship between these two groups is not fully known yet.

5. Appendix

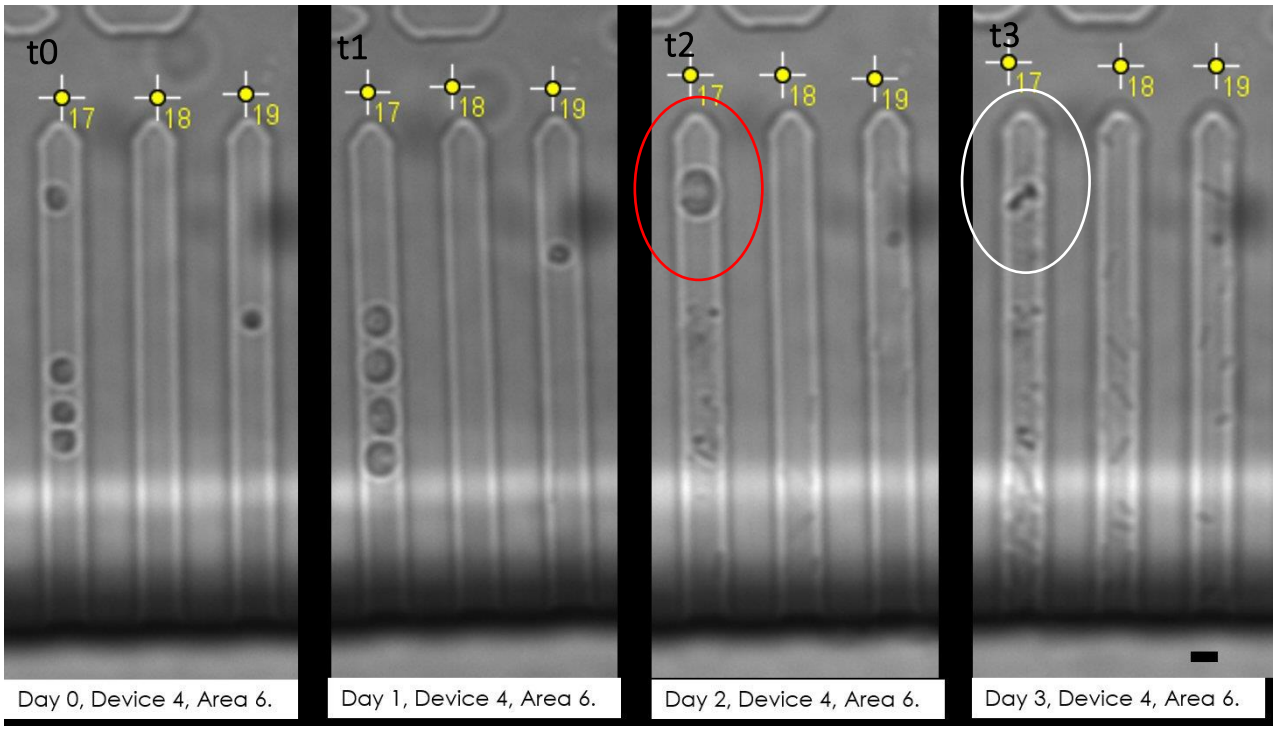

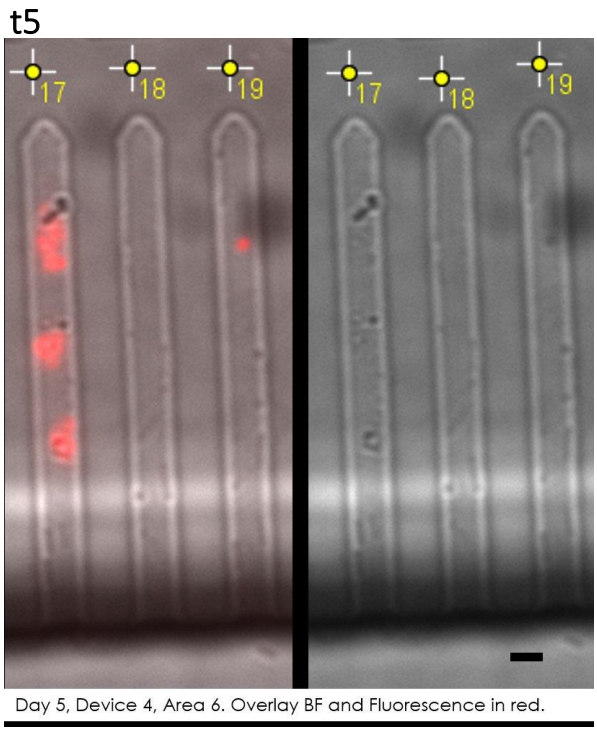

Figure 24. *Development of* O. tauri *within the Modified Mother Machine device 4. Area 6. Yellow numbers are markers. Scale bars are all 1 μm. This specific channels presented a different development to some extent. Initial number of cells was 4 for the arm no. 17. The growth of the 4 cells is observable, but by day 2, only one is intact (red circle). Yet, in the next day (t= 3) this cell also degraded, being only clearly visible two black dots (white circle). Notwithstanding, the last day, all the initial cells presented auto-fluorescence (in red), suggesting that either the chloroplast was kept undamaged or that the cells were alive.*

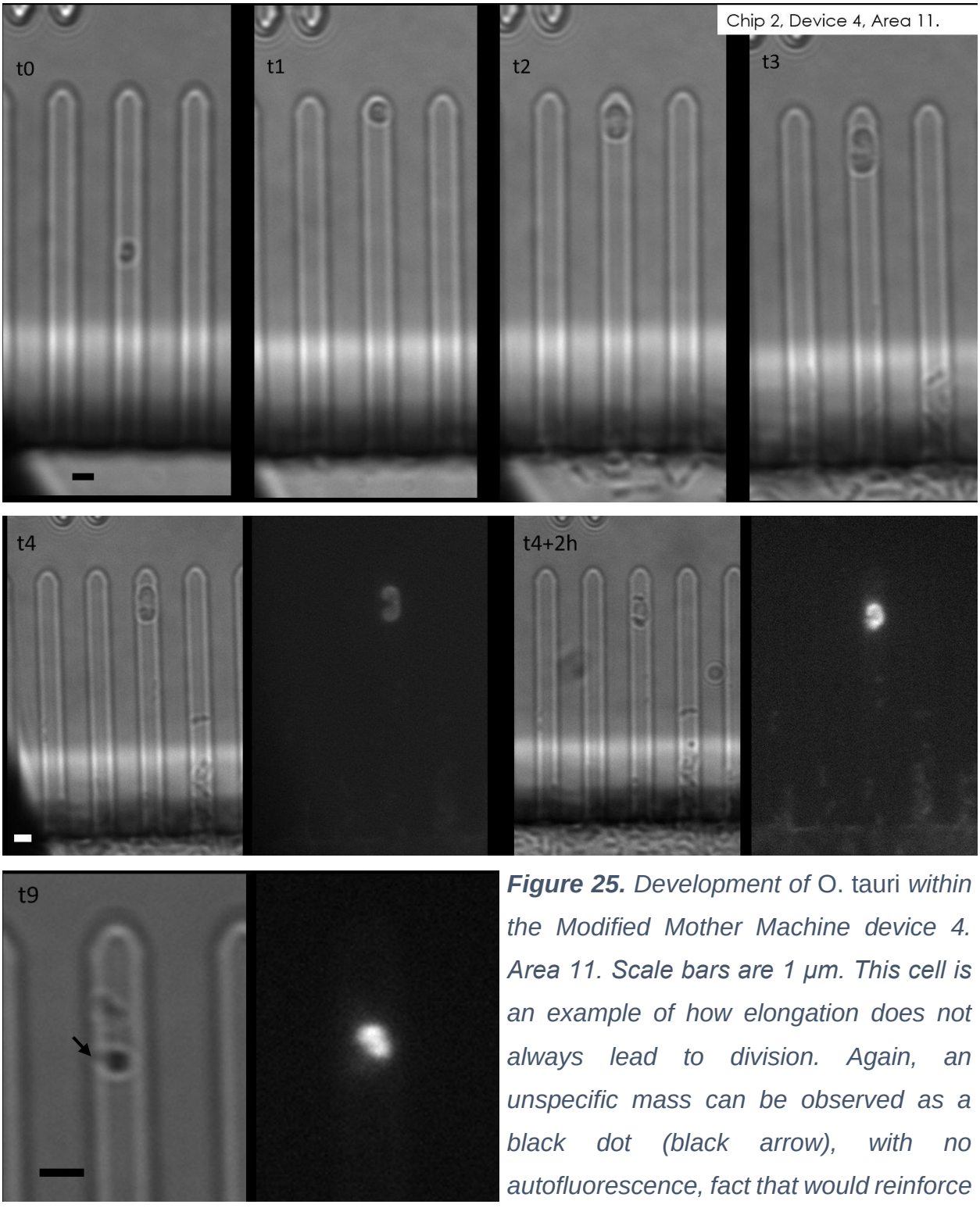

Figure 25. *Development of* O. tauri *within the Modified Mother Machine device 4. Area 11. Scale bars are 1 µm. This cell is an example of how elongation does not always lead to division. Again, an unspecific mass can be observed as a black dot (black arrow), with no autofluorescence, fact that would reinforce the idea of it being a starch granule.*

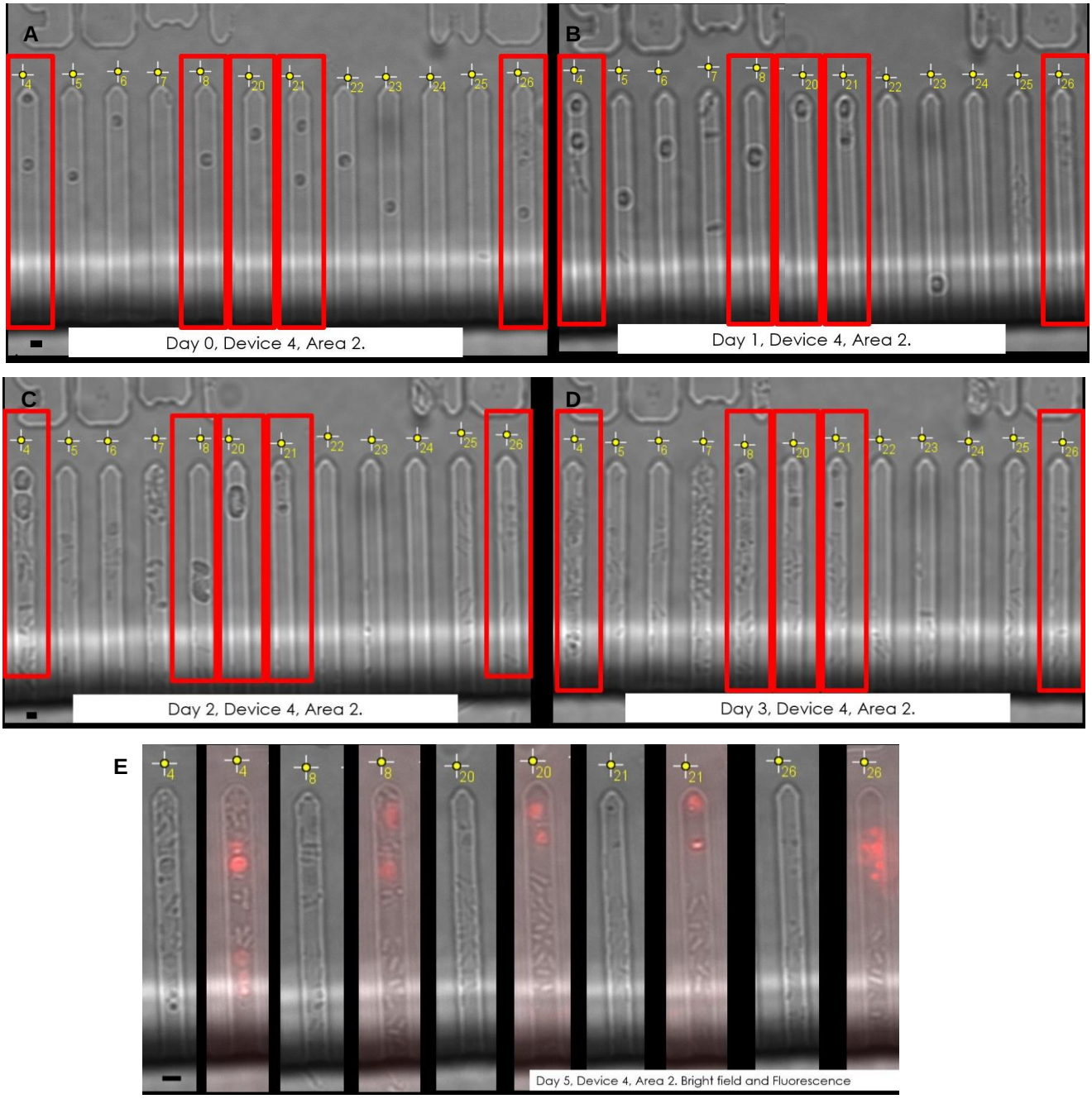

Figure 26. *Development of* O. tauri *within the Modified Mother Machine device 4. Area 2. Yellow numbers are markers. Scale bars are all 1 µm. In this area, O. tauri development was similar to that found in Area 1. In this, both phenomenon were observed: algal cells grew in size (t= 1,* ***B****) and the elongation of the cells (t= 2,* ***C****).*

*However, for t= 3 (**D**), cells were not found in any of the latter aspects, instead, appearance of the circular shapes happened, as well as the proliferation of bacteria.By day 5 (**E**), arms 14, 18, 20 divided. Channel no. 26 was followed due to the exceptional shapes seen in t=0, whose shape barely changed during the 5 days.*

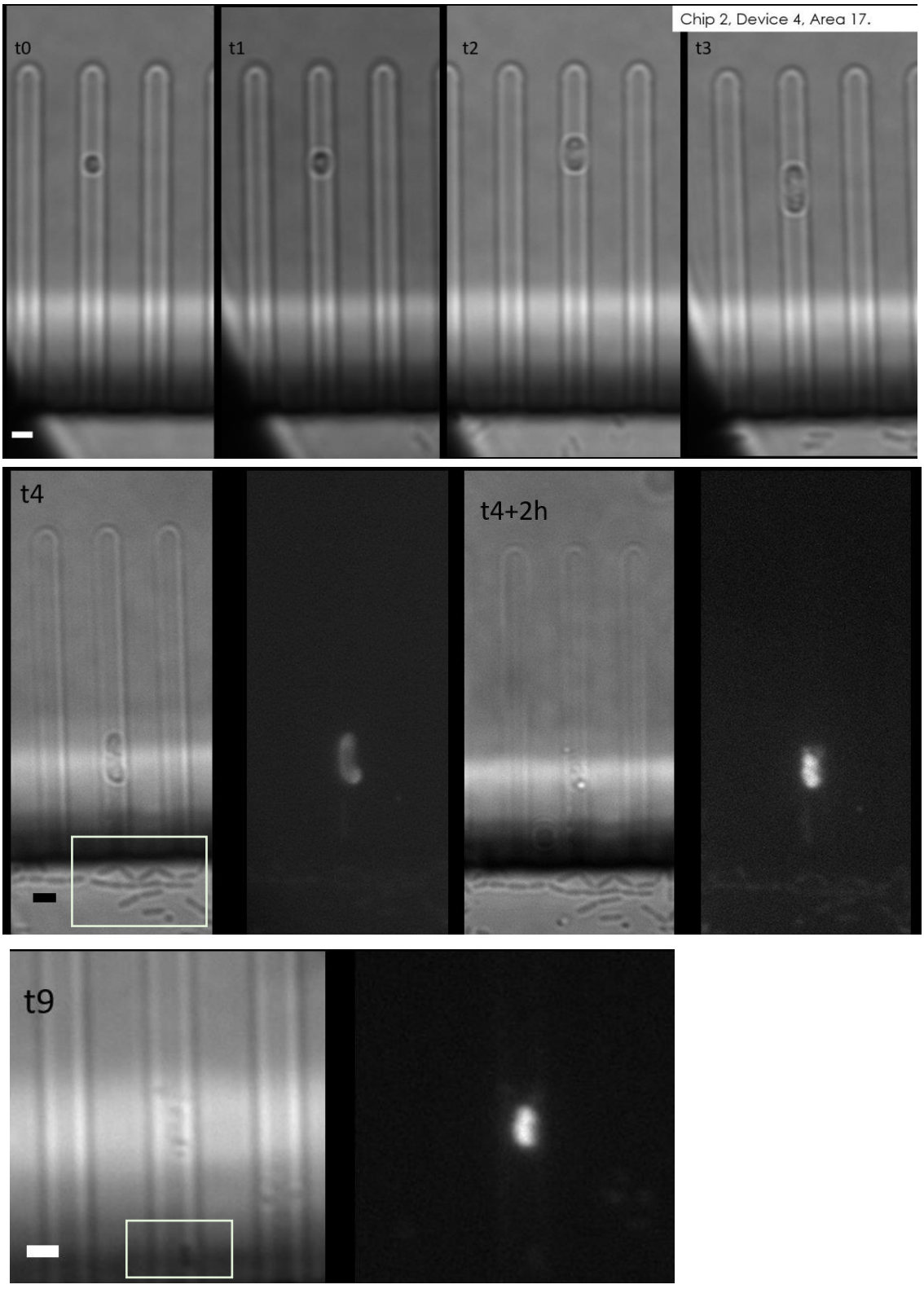

Figure 27. *Development of* O. tauri *within the Modified Mother Machine device 4. Area 17. Scale bars are 1 µm.*

In this example, it can be observed how the cell is sliding down the arm as it elongates. At the same time, bacteria is starting to grow at the entrance of the arm (light-green quadrangles).

6. Bibliography

Abby, S. *et al.* (2014) 'Bacteria in Ostreococcus tauri cultures - friends, foes or hitchhikers?', *Frontiers in Microbiology*, 5(SEP). doi:10.3389/fmicb.2014.00505.

Andar, A.U. *et al.* (2019) 'Low-cost customizable microscale toolkit for rapid screening and purification of therapeutic proteins', *Biotechnology and Bioengineering*, 116(4), pp. 870–881. doi:10.1002/bit.26876.

Anderson, R.A. (2005) *Algal Culturing Techniques, 1st Edition*, *Journal of Chemical Information and Modeling*. Available at: https://www.elsevier.com/books/algal-culturing-techniques/andersen/978-0-12-088426-1 (Accessed: 16 August 2021).

Baltekin, Ö. *et al.* (2017) 'Antibiotic susceptibility testing in less than 30 min using direct single-cell imaging', *Proceedings of the National Academy of Sciences of the United States of America*, 114(34), pp. 9170–9175. doi:10.1073/pnas.1708558114.

Bamford, R.A. *et al.* (2017) 'Investigating the physiology of viable but non-culturable bacteria by microfluidics and time-lapse microscopy', *BMC Biology*, 15(1), p. 121. doi:10.1186/s12915-017-0465-4.

Banerjee, S., Ray, A. and Das, D. (2021) 'Optimization of Chlamydomonas reinhardtii cultivation with simultaneous CO2 sequestration and biofuels production in a biorefinery framework', *Science of The Total Environment*, 762, p. 143080. doi:10.1016/J.SCITOTENV.2020.143080.

Bar-On, Y.M., Phillips, R. and Milo, R. (2018) 'The biomass distribution on Earth', *Proceedings of the National Academy of Sciences of the United States of America*, 115(25), pp. 6506–6511. doi:10.1073/pnas.1711842115.

Beebe, D.J., Mensing, G.A. and Walker, G.M. (2002) 'Physics and applications of microfluidics in biology', *Annual Review of Biomedical Engineering*, pp. 261–286. doi:10.1146/annurev.bioeng.4.112601.125916.

Birkhofer, K. *et al.* (2018) 'Relationships between multiple biodiversity components and ecosystem services along a landscape complexity gradient', *Biological Conservation*, 218(November 2017), pp. 247–253. doi:10.1016/j.biocon.2017.12.027.

Bodénès, P. *et al.* (2019) 'Microfluidic techniques for enhancing biofuel and biorefinery industry based on microalgae', *Biotechnology for Biofuels*, 12(1), p. 33. doi:10.1186/s13068-019-1369-z.

Boon, E. *et al.* (2014) 'Interactions in the microbiome: communities of organisms and communities of genes', *FEMS Microbiology Reviews*, 38(1), pp. 90–118. doi:10.1111/1574-6976.12035.

Burmeister, A. and Grünberger, A. (2020) 'Microfluidic cultivation and analysis tools for interaction studies of microbial co-cultures', *Current Opinion in Biotechnology*. Elsevier Ltd, pp. 106–115. doi:10.1016/j.copbio.2019.09.001.

Cama, J. *et al.* (2020) 'Single-cell microfluidics facilitates the rapid quantification of antibiotic accumulation in Gram-negative bacteria', *Lab on a Chip*, 20(15), pp. 2765–2775. doi:10.1039/D0LC00242A.

Castaldello, C. *et al.* (2019) 'Microfluidic Platform for Microalgae Cultivation under Non-limiting CO 2 Conditions'. doi:10.1021/acs.iecr.9b02888.

Chartier, T.F. *et al.* (2018) 'Whole-head recording of chemosensory activity in the marine annelid Platynereis dumerilii', *Royal Society Open Biology*, 8(10). doi:10.1098/RSOB.180139.

Chiu, D.T. *et al.* (2017) 'Small but Perfectly Formed? Successes, Challenges, and Opportunities for Microfluidics in the Chemical and Biological Sciences', *Chem*. Elsevier Inc, pp. 201–223. doi:10.1016/j.chempr.2017.01.009.

Choi, T.-Y. *et al.* (2021) 'Zebrafish as an animal model for biomedical research', *Experimental & Molecular Medicine 2021 53:3*, 53(3), pp. 310–317. doi:10.1038/s12276-021-00571-5.

Chretiennot-Dinet, M.J. *et al.* (1995) 'A new marine picoeucaryote: Ostreococcus tauri gen. et sp. nov. (Chlorophyta, Prasinophyceae)', *Phycologia*, 34(4), pp. 285–292. doi:10.2216/i0031-8884-34-4-285.1.

Clerissi, C., Desdevises, Y. and Grimsley, N. (2012) 'Prasinoviruses of the Marine Green Alga Ostreococcus tauri Are Mainly Species Specific', *Journal of Virology*, 86(8), pp.

4611–4619. doi:10.1128/jvi.07221-11.

Convery, N. and Gadegaard, N. (2019) ‘30 years of microfluidics’, *Micro and Nano Engineering*. Elsevier B.V., pp. 76–91. doi:10.1016/j.mne.2019.01.003.

Cooper, M.B. *et al.* (2019) ‘Cross-exchange of B-vitamins underpins a mutualistic interaction between Ostreococcus tauri and Dinoroseobacter shibae’, *ISME Journal*, 13(2), pp. 334–345. doi:10.1038/s41396-018-0274-y.

Costello, M.J. and Breyer, S. (2017) ‘Ocean Depths: The Mesopelagic and Implications for Global Warming’, *Current Biology*, 27(1), pp. R36–R38. doi:10.1016/J.CUB.2016.11.042.

Deng, Y., Guo, Y. and Xu, B. (no date) ‘processes Recent Development of Microfluidic Technology for Cell Trapping in Single Cell Analysis: A Review’. doi:10.3390/pr8101253.

Depauw, F.A. *et al.* (2012) ‘Exploring the molecular basis of responses to light in marine diatoms’, *Journal of Experimental Botany*, 63(4), pp. 1575–1591. doi:10.1093/JXB/ERS005.

Dervisevic, E. *et al.* (2019) ‘Recent progress in lab-on-a-chip systems for the monitoring of metabolites for mammalian and microbial cell research’, *Sensors (Switzerland)*. MDPI AG. doi:10.3390/s19225027.

Dimitriu, T. *et al.* (2022) ‘Bacteriostatic antibiotics promote CRISPR-Cas adaptive immunity by enabling increased spacer acquisition’, *Cell Host & Microbe*, 30(1), pp. 31-40.e5. doi:10.1016/J.CHOM.2021.11.014.

Donachie, S.P. *et al.* (2021) ‘The problem with “microbiome”’, *Diversity*, 13(4). doi:10.3390/D13040138.

Duffy, D.C. *et al.* (1998) ‘Rapid prototyping of microfluidic systems in poly(dimethylsiloxane)’, *Analytical Chemistry*, 70(23), pp. 4974–4984. doi:10.1021/ac980656z.

European Commission (2021) *Special Eurobarometer 513: Climate Change*. Available at: https://www.europa.eu/eurobarometer.

Farinas, B. *et al.* (2006) 'Natural synchronisation for the study of cell division in the green unicellular alga Ostreococcus tauri', *Plant Molecular Biology*, 60(2), pp. 277–292. doi:10.1007/s11103-005-4066-1.

Finkel, Z. V. *et al.* (2010) 'Phytoplankton in a changing world: Cell size and elemental stoichiometry', *Journal of Plankton Research*. Oxford Academic, pp. 119–137. doi:10.1093/plankt/fbp098.

Fredrickson, C.K. and Fan, Z.H. (2004) 'Macro-to-micro interfaces for microfluidic devices', *Lab on a Chip*. Royal Society of Chemistry, pp. 526–533. doi:10.1039/b410720a.

Frenkel, J., Vyverman, W. and Pohnert, G. (2014) 'Small molecules: from structural diversity to signalling and regulatory roles Pheromone signaling during sexual reproduction in algae'. doi:10.1111/tpj.12496.

Frenzel, W. and McKelvie, I.D. (2008) 'Photometry', *Comprehensive Analytical Chemistry*, 54, pp. 311–342. doi:10.1016/S0166-526X(08)00612-0.

Fuentes, J.L. *et al.* (2016) 'Impact of microalgae-bacteria interactions on the production of algal biomass and associated compounds', *Marine Drugs*, 14(5). doi:10.3390/md14050100.

Funfak, A. *et al.* (2007) 'Micro fluid segment technique for screening and development studies on Danio rerio embryos', *Lab on a Chip*, 7(9), pp. 1132–1138. doi:10.1039/b701116d.

Gale, B.K. *et al.* (2008) 'Low-Cost MEMS Technologies', *Comprehensive Microsystems*, 1, pp. 341–378. doi:10.1016/B978-044452190-3.00011-2.

Garcia-Pichel, F. *et al.* (2009) 'Estimates of global cyanobacterial biomass and its distribution', *Algological Studies*, 109(1), pp. 213–227. doi:10.1127/1864-1318/2003/0109-0213.

Gilroy, R. *et al.* (2021) 'Extensive microbial diversity within the chicken gut microbiome revealed by metagenomics and culture', *PeerJ*, 9. doi:10.7717/PEERJ.10941.

Glover, G. *et al.* (2022) 'Nutrient and salt depletion synergistically boosts glucose metabolism in individual Escherichia coli cells', *Communications Biology 2022 5:1*, 5(1), pp. 1–14. doi:10.1038/s42003-022-03336-6.

Golden, J.P. *et al.* (2009) 'Multi-wavelength microflow cytometer using groove-generated sheath flow', *Lab on a chip*, 9(13), p. 1942. doi:10.1039/B822442K.

Goode, O. *et al.* (2021) 'Heterologous Protein Expression Favors the Formation of Protein Aggregates in Persister and Viable but Nonculturable Bacteria', *ACS Infectious Diseases*, 7(6), pp. 1848–1858. doi:10.1021/ACSINFECDIS.1C00154/SUPPL_FILE/ID1C00154_SI_001.PDF.

Gouda, M. (2021) 'Recent Innovations of Microalgae Single Cell Phytochemical Studies Recent Innovations of Microalgae Single Cell Phytochemical Studies', (June). doi:10.32474/AOICS.2021.05.000203.

Griffiths, M.J. *et al.* (2011) 'Interference by pigment in the estimation of microalgal biomass concentration by optical density', *Journal of Microbiological Methods*, 85(2), pp. 119–123. doi:10.1016/j.mimet.2011.02.005.

Hakim, S. *et al.* (2021) 'Rhizosphere Engineering With Plant Growth-Promoting Microorganisms for Agriculture and Ecological Sustainability', *Frontiers in Sustainable Food Systems*, 0, p. 16. doi:10.3389/FSUFS.2021.617157.

Hammond, K. *et al.* (2021) 'Switching Cytolytic Nanopores into Antimicrobial Fractal Ruptures by a Single Side Chain Mutation', *ACS Nano*, 15(6), pp. 9679–9689. doi:10.1021/ACSNANO.1C00218/SUPPL_FILE/NN1C00218_SI_002.AVI.

Hashemi, N. *et al.* (2011) 'Optofluidic characterization of marine algae using a microflow cytometer', *Biomicrofluidics*, 5(3), p. 032009. doi:10.1063/1.3608136.

Henderson, G.P., Gan, L. and Jensen, G.J. (2007) '3-D Ultrastructure of O. tauri: Electron Cryotomography of an Entire Eukaryotic Cell', *PLoS ONE*, 2(1). doi:10.1371/journal.pone.0000749.

Hildebrand, M. *et al.* (2016) 'Applications of imaging flow cytometry for microalgae', *Methods in Molecular Biology*, 1389, pp. 47–67. doi:10.1007/978-1-4939-3302-0_4.

Hodzic, E. (2016) ‘Single-cell analysis: Advances and future perspectives’, *Bosnian Journal of Basic Medical Sciences*, 16(4), p. 313. doi:10.17305/BJBMS.2016.1371.

Hong, J.W., Song, S. and Shin, J.H. (2013) ‘A novel microfluidic co-culture system for investigation of bacterial cancer targeting’, *Lab on a Chip*, 13(15), pp. 3033–3040. doi:10.1039/C3LC50163A.

Houliez, E. *et al.* (2012) ‘Spectral fluorometric characterization of Haptophyte dynamics using the FluoroProbe: an application in the eastern English Channel for monitoring Phaeocystis globosa’, *Journal of Plankton Research*, 34(2), pp. 136–151. doi:10.1093/PLANKT/FBR091.

Huebner, A. *et al.* (2007) ‘Quantitative detection of protein expression in single cells using droplet microfluidics’, *Chemical Communications*, (12), pp. 1218–1220. doi:10.1039/B618570C.

Hwang, H. and Lu, H. (2013) ‘Microfluidic tools for developmental studies of small model organisms -nematodes, fruit flies, and zebrafish’, *Biotechnology Journal*, 8(2), pp. 192–205. doi:10.1002/biot.201200129.

Islam, M.S. and Kieu, E. (2021) ‘Sociological perspectives on climate change and society: A review’, *Climate*, 9(1), pp. 1–14. doi:10.3390/cli9010007.

Jeffrey S. Levinton (1995) *Marine Biology: Function, Biodiversity and Ecology.* 2nd, 2001st edn. Oxford University Press.

Jo, M.C. and Qin, L. (2016) ‘Microfluidic Platforms for Yeast-Based Aging Studies’, *Small*. Wiley-VCH Verlag, pp. 5787–5801. doi:10.1002/smll.201602006.

Kaiser, M. *et al.* (2018) ‘Monitoring single-cell gene regulation under dynamically controllable conditions with integrated microfluidics and software’, *Nature Communications 2018 9:1*, 9(1), pp. 1–16. doi:10.1038/s41467-017-02505-0.

Kazamia, E. *et al.* (2012) ‘Mutualistic interactions between vitamin B12-dependent algae and heterotrophic bacteria exhibit regulation’, *Environmental Microbiology*, 14(6), pp. 1466–1476. doi:10.1111/j.1462-2920.2012.02733.x.

Khalili, A. and Rezai, P. (2019a) ‘Microfluidic devices for embryonic and larval zebrafish studies’, *Briefings in Functional Genomics*, 18(6), pp. 419–432. doi:10.1093/bfgp/elz006.

Kim, B.H. *et al.* (2014) ‘Role of Rhizobium, a plant growth promoting bacterium, in enhancing algal biomass through mutualistic interaction’, *Biomass and Bioenergy*, 69, pp. 95–105. doi:10.1016/j.biombioe.2014.07.015.

Kim, H.S., Devarenne, T.P. and Han, A. (2018) ‘Microfluidic systems for microalgal biotechnology: A review Keywords: Microalgae Cyanobacteria Microfluidics Lab-on-a-chip Biofuel Microfabricated systems’. doi:10.1016/j.algal.2017.11.020.

Kremp, A. *et al.* (2012) ‘Intraspecific variability in the response of bloom-forming marine microalgae to changed climate conditions’, *Ecology and Evolution*, 2(6), pp. 1195–1207. doi:10.1002/ece3.245.

Krohn-Molt, I. *et al.* (2017) ‘Insights into Microalga and Bacteria Interactions of Selected Phycosphere Biofilms Using Metagenomic, Transcriptomic, and Proteomic Approaches’, *Frontiers in Microbiology*, 8(OCT), p. 1941. doi:10.3389/fmicb.2017.01941.

Kukurba, K.R. and Montgomery, S.B. (2015) ‘RNA Sequencing and Analysis’, *Cold Spring Harbor protocols*, 2015(11), p. 951. doi:10.1101/PDB.TOP084970.

Łapińska, U. *et al.* (2019) ‘Bacterial ageing in the absence of external stressors’, *Philosophical Transactions of the Royal Society B: Biological Sciences*, 374(1786), p. 20180442. doi:10.1098/rstb.2018.0442.

Łapińska, U. *et al.* (2021) ‘Fast bacterial growth reduces antibiotic accumulation and efficacy’, *bioRxiv*, p. 2021.10.18.464851. doi:10.1101/2021.10.18.464851.

Lasken, R.S. and McLean, J.S. (2014) ‘Recent advances in genomic DNA sequencing of microbial species from single cells’, *Nature reviews. Genetics*, 15(9), p. 577. doi:10.1038/NRG3785.

Lelandais, G. *et al.* (2016) ‘Ostreococcus tauri is a new model green alga for studying iron metabolism in eukaryotic phytoplankton’, *BMC Genomics*, 17(1). doi:10.1186/S12864-016-2666-6.

Lombard, F. *et al.* (2019) 'Globally Consistent Quantitative Observations of Planktonic Ecosystems', *Frontiers in Marine Science*, 0(MAR), p. 196. doi:10.3389/FMARS.2019.00196.

Longford, S.R. *et al.* (2019) 'Interactions within the microbiome alter microbial interactions with host chemical defences and affect disease in a marine holobiont', *Scientific Reports 2019 9:1*, 9(1), pp. 1–13. doi:10.1038/s41598-018-37062-z.

Luke, C.S. *et al.* (2016) 'A Microfluidic Platform for Long-Term Monitoring of Algae in a Dynamic Environment', *ACS Synthetic Biology*, 5(1), pp. 8–14. doi:10.1021/acssynbio.5b00094.

MacIntyre, H.L., Lawrenz, E. and Richardson, T.L. (2010) 'Taxonomic Discrimination of Phytoplankton by Spectral Fluorescence', *Chlorophyll a Fluorescence in Aquatic Sciences: Methods and Applications*, pp. 129–169. doi:10.1007/978-90-481-9268-7_7.

Mandy, F.F., Bergeron, M. and Minkus, T. (1995) 'Principles of flow cytometry', *Transfusion Science*, 16(4), pp. 303–314. doi:10.1016/0955-3886(95)00041-0.

Massalha, H. *et al.* (2017) 'Live imaging of root–bacteria interactions in a microfluidics setup', *Proceedings of the National Academy of Sciences*, 114(17), pp. 4549–4554. doi:10.1073/PNAS.1618584114.

Massana, R. (2011) 'Eukaryotic Picoplankton in Surface Oceans', *Annual Review of Microbiology*, 65(1), pp. 91–110. doi:10.1146/annurev-micro-090110-102903.

Michalec, F.-G. *et al.* (2017) 'Zooplankton can actively adjust their motility to turbulent flow', *Proceedings of the National Academy of Sciences of the United States of America*, 114(52), p. E11199. doi:10.1073/PNAS.1708888114.

Mielańczyk, Ł., Matysiak, N. and Wojnicz, O.K. and R. (2015) 'Transmission Electron Microscopy of Biological Samples', *The Transmission Electron Microscope - Theory and Applications* [Preprint]. doi:10.5772/60680.

Monier, A., Worden, A.Z. and Richards, T.A. (2016) 'Phylogenetic diversity and biogeography of the Mamiellophyceae lineage of eukaryotic phytoplankton across the oceans', *Environmental Microbiology Reports*, 8(4), pp. 461–469. doi:10.1111/1758-

2229.12390.

Nash, K.L. *et al.* (2021) ‘Oceans and society: feedbacks between ocean and human health’, *Reviews in Fish Biology and Fisheries 2021 32:1*, 32(1), pp. 161–187. doi:10.1007/S11160-021-09669-5.

Nations, T.U. (2021) *The Ocean Decade at COP26*, *Https://Www.Oceandecade.Org/*. Available at: https://www.oceandecade.org/vision-mission/ (Accessed: 2 April 2022).

Nguyen, T. *et al.* (2019) ‘micromachines A Complete Protocol for Rapid and Low-Cost Fabrication of Polymer Microfluidic Chips Containing Three-Dimensional Microstructures Used in Point-of-Care Devices’. doi:10.3390/mi10090624.

Orellana, M. V *et al.* (2013) ‘A Role for Programmed Cell Death in the Microbial Loop’, *PLoS ONE*, 8(5), p. 62595. doi:10.1371/journal.pone.0062595.

Osmekhina, E. *et al.* (2018) ‘Controlled communication between physically separated bacterial populations in a microfluidic device’, *Communications Biology 2018 1:1*, 1(1), pp. 1–7. doi:10.1038/s42003-018-0102-y.

Pachiadaki, M.G. *et al.* (2019) ‘Charting the Complexity of the Marine Microbiome through Single-Cell Genomics’, *Cell*, 179(7), pp. 1623-1635.e11. doi:10.1016/J.CELL.2019.11.017.

Pernice, M.C. *et al.* (2014) ‘Global abundance of planktonic heterotrophic protists in the deep ocean’, *The ISME Journal 2015 9:3*, 9(3), pp. 782–792. doi:10.1038/ismej.2014.168.

Pomeroy, L.R. (1974) ‘The ocean’s food web, a changing paradigm’, *BioScience*, 24(9), pp. 499–504. doi:10.2307/1296885.

Pomeroy, L.R. *et al.* (2007) ‘The microbial loop’, *Oceanography*, 20(SPL.ISS. 2), pp. 28–33. doi:10.5670/oceanog.2007.45.

Ral, J.P. *et al.* (2004) ‘Starch division and partitioning. A mechanism for granule propagation and maintenance in the picophytoplanktonic green alga Ostreococcus tauri.’, *Plant physiology*, 136(2), pp. 3333–3340. doi:10.1104/pp.104.044131.

Ramanan, R. *et al.* (2015) 'Phycosphere bacterial diversity in green algae reveals an apparent similarity across habitats', *Algal Research*, 8, pp. 140–144. doi:10.1016/j.algal.2015.02.003.

Ramanan, R. *et al.* (2016) 'Algae-bacteria interactions: Evolution, ecology and emerging applications', *Biotechnology Advances*. Elsevier Inc., pp. 14–29. doi:10.1016/j.biotechadv.2015.12.003.

Ramanathan, N. *et al.* (2013) *Ocean on a chip: Microfluidics as a gateway to functional marine ecology*, *17th International Conference on Miniaturized Systems for Chemistry and Life Sciences, MicroTAS 2013*. Available at: http://www.anc.ed.ac.uk/demos/tracker/ (Accessed: 20 March 2020).

Ramanathan, N. *et al.* (2015) 'Quantifying preferences and responsiveness of marine zooplankton to changing environmental conditions using microfluidics', *PLoS ONE*, 10(10). doi:10.1371/JOURNAL.PONE.0140553.

Reinmets, K. *et al.* (2019) 'Microfluidic quantification and separation of yeast based on surface adhesion', *Lab on a Chip*, 19(20), pp. 3481–3489. doi:10.1039/c9lc00275h.

Rodrigues, R.V., Patil, J.S. and Anil, A.C. (2022) 'Dinoflagellates cyst assemblage concerning trophic index for eutrophication from major ports along the west coast of India', *Marine Pollution Bulletin*, 176, p. 113423. doi:10.1016/J.MARPOLBUL.2022.113423.

Rosenauer, M. *et al.* (2010) 'Miniaturized flow cytometer with 3D hydrodynamic particle focusing and integrated optical elements applying silicon photodiodes', *Microfluidics and Nanofluidics 2010 10:4*, 10(4), pp. 761–771. doi:10.1007/S10404-010-0707-Z.

Rusconi, R., Garren, M. and Stocker, R. (2014) 'Microfluidics Expanding the Frontiers of Microbial Ecology'. doi:10.1146/annurev-biophys-051013-022916.

Sato, H. *et al.* (2007) '3D sheath flow using hydrodynamic position control of the sample flow', *Journal of Micromechanics and Microengineering*, 17(11), pp. 2211–2216. doi:10.1088/0960-1317/17/11/006.

Schaap, A., Rohrlack, T. and Bellouard, Y. (2012) 'Optical classification of algae species with a glass lab-on-a-chip', *Lab on a Chip*, 12(8), pp. 1527–1532.

doi:10.1039/C2LC21091F.

Scranton, M.A. *et al.* (2015) 'Chlamydomonas as a model for biofuels and bio-products production', *Plant Journal*, 82(3), pp. 523–531. doi:10.1111/tpj.12780.

Sebastián, M. and Gasol, J.M. (2019) 'Visualization is crucial for understanding microbial processes in the ocean', *Philosophical Transactions of the Royal Society B: Biological Sciences*, 374(1786). doi:10.1098/rstb.2019.0083.

Seymour, J.R. *et al.* (2010) 'Chemoattraction to Dimethylsulfoniopropionate Throughout the Marine Microbial Food Web', *Science*, 329(5989), pp. 342–345. doi:10.1126/SCIENCE.1188418.

Seymour, J.R. *et al.* (2017) 'Zooming in on the phycosphere: The ecological interface for phytoplankton-bacteria relationships', *Nature Microbiology*. Nature Publishing Group. doi:10.1038/nmicrobiol.2017.65.

Simcock, A. *et al.* (2021) *Global Ocean Science Report 2020*, *Global Ocean Science Report 2020*. doi:10.18356/9789216040048.

Single-cell microbiology (2016) *Nature Biotechnology*. doi:10.1038/nbt.3728.

Son, K., Brumley, D.R. and Stocker, R. (2015) 'Live from under the lens: exploring microbial motility with dynamic imaging and microfluidics', *Nature Reviews Microbiology 2015 13:12*, 13(12), pp. 761–775. doi:10.1038/nrmicro3567.

Spencer, D. and Morgan, H. (2011) 'Positional dependence of particles in microfludic impedance cytometry', *Lab on a Chip*, 11(7), pp. 1234–1239. doi:10.1039/C1LC20016J.

Sullivan, C. *et al.* (2021) 'Modeling Virus-Induced Inflammation in Zebrafish: A Balance Between Infection Control and Excessive Inflammation', *Frontiers in Immunology*, 0, p. 1635. doi:10.3389/FIMMU.2021.636623.

Tang, B. *et al.* (2015) 'Web resources for model organism studies', *Genomics, Proteomics and Bioinformatics*. Beijing Genomics Institute, pp. 64–68. doi:10.1016/j.gpb.2015.01.003.

Temiz, Y. *et al.* (2015) 'Lab-on-a-chip devices: How to close and plug the lab?',

Microelectronic Engineering. Elsevier, pp. 156–175. doi:10.1016/j.mee.2014.10.013.

Terry, S.C., Herman, J.H. and Angell, J.B. (1979) 'A Gas Chromatographic Air Analyzer Fabricated on a Silicon Wafer', *IEEE Transactions on Electron Devices*, 26(12), pp. 1880–1886. doi:10.1109/T-ED.1979.19791.

Toutain, P.-L., Ferran, A. and Bousquet-Mélou, A. (2010) 'Species Differences in Pharmacokinetics and Pharmacodynamics', *Handbook of Experimental Pharmacology*, 199, pp. 19–48. doi:10.1007/978-3-642-10324-7_2.

US Department of Commerce, N.O. and A.A. (2018) *30 Days of the Ocean*. Available at: https://oceanservice.noaa.gov/news/june14/30days.html (Accessed: 29 March 2022).

Variem, S.S. and Kizhakkedath, V.K. (2021) 'Phycosphere associated bacteria; a prospective source of bioactive compounds', *Biologia*, 76(3), pp. 1095–1098. doi:10.2478/s11756-020-00640-6.

Vembadi, A., Menachery, A. and Qasaimeh, M.A. (2019) 'Cell Cytometry: Review and Perspective on Biotechnological Advances', *Frontiers in Bioengineering and Biotechnology*, 0(JUN), p. 147. doi:10.3389/FBIOE.2019.00147.

Venuleo, M., Raven, J.A. and Giordano, M. (2017) 'Intraspecific chemical communication in microalgae', *New Phytologist*, 215(2), pp. 516–530. doi:10.1111/NPH.14524.

Wang, J. *et al.* (2016) 'Detection of activity of single microalgae cells in a new microfluidic cell capturing chip', *Measurement Science and Technology*, 27(12), p. 125701. doi:10.1088/0957-0233/27/12/125701.

Wang, P. *et al.* (2010) 'Report Robust Growth of Escherichia coli', *Current Biology*, 20, pp. 1099–1103. doi:10.1016/j.cub.2010.04.045.

Westerwalbesloh, C. *et al.* (2019) 'A microfluidic photobioreactor for simultaneous observation and cultivation of single microalgal cells or cell aggregates', *PLoS ONE*, 14(4). doi:10.1371/journal.pone.0216093.

White, A.R., Jalali, M. and Sheng, J. (no date) 'A new ecology-on-a-chip microfluidic platform to study interactions of microbes with a rising oil droplet'. doi:10.1038/s41598-

019-50153-9.

Wirtz, K. and Smith, S.L. (2020) ‘Vertical migration by bulk phytoplankton sustains biodiversity and nutrient input to the surface ocean’, *Scientific Reports 2020 10:1*, 10(1), pp. 1–12. doi:10.1038/s41598-020-57890-2.

Worden, A.Z. *et al.* (2015) ‘Rethinking the marine carbon cycle: Factoring in the multifarious lifestyles of microbes’, *Science*, 347(6223). doi:10.1126/SCIENCE.1257594.

Xiao, L., Liu, J. and Ge, J. (2021) ‘Dynamic game in agriculture and industry cross-sectoral water pollution governance in developing countries’, *Agricultural Water Management*, 243, p. 106417. doi:10.1016/J.AGWAT.2020.106417.

Yang, D. *et al.* (2018) ‘Analysis of factors limiting bacterial growth in PDMS mother machine devices’, *Frontiers in Microbiology*, 9(MAY). doi:10.3389/fmicb.2018.00871.

Yang, L. *et al.* (2018) ‘Growth and lipid accumulation by different nutrients in the microalga Chlamydomonas reinhardtii’, *Biotechnology for Biofuels 2018 11:1*, 11(1), pp. 1–12. doi:10.1186/S13068-018-1041-Z.

Zhang, B. *et al.* (2020) ‘Microalgal-bacterial consortia: From interspecies interactions to biotechnological applications’, *Renewable and Sustainable Energy Reviews*. Elsevier Ltd, p. 109563. doi:10.1016/j.rser.2019.109563.

Zhang, X.-H. *et al.* (2021) ‘Viable but nonculturable bacteria and their resuscitation: implications for cultivating uncultured marine microorganisms’, 3, pp. 189–203. doi:10.1007/s42995-020-00041-3.

Zhu, F. *et al.* (2014) ‘Fishing on chips: Up-and-coming technological advances in analysis of zebrafish and Xenopus embryos’, *Cytometry Part A*. Wiley-Liss Inc., pp. 921–932. doi:10.1002/cyto.a.22571.

Zhu, F. *et al.* (2015) ‘Three-dimensional printed millifluidic devices for zebrafish embryo tests’, *Biomicrofluidics*, 9(4). doi:10.1063/1.4927379.